

# Synthesis, Characterization and Spectroscopic Study of New Metal Complexes form Heterocyclic Compounds for Photostability Study

Ali M. A. Al-Khazraji<sup>1\*</sup>, Rehab A. M. Al Hassani<sup>2</sup>

<sup>1</sup>Department of Chemistry, College of Education for Pure Sciences / Ibn al-Haytham, University of Baghdad, <sup>2</sup>Baghdad, Iraq, <sup>b</sup>Department of Chemistry, College of Science, Mustansirya University, Baghdad, Iraq.

\*Corresponding author: [alimudher82@gmail.com](mailto:alimudher82@gmail.com)

Article History:

Submitted: 23.03.2020

Revised: 15.05.2020

Accepted: 24.06.2020

## ABSTRACT

In present project, new Schiff base of 4, 4'-(((1E, 1'E)-1,4-phenylenebis-(methane-ylidene))-bis-(azane-ylidene)) bis-(5-(4-chlorophenyl)-4H-1,2,4-triazole-3-thione) (L<sub>3</sub>) has been synthesized by condensation of 4-amino-5-(4-chlorophenyl)-2,4-dihydro-3H-1,2,4-triazole-3-thione with benzene-1,4-dicarboxaldehyde. The new asymmetrical Schiff base (L<sub>3</sub>) used as a ligand to synthesize a new complex with Co(II), Ni(II), Cu(II), Pd(II), and Pt(IV) metal ions by 1:2 (Metal: ligand) ratio. New ligand and their complexes have been examined and Confirmed by Fourier-transform infrared (FT-IR), Ultraviolet-visible (UV-visible), Proton nuclear magnetic resonance (1H NMR), carbon13 nuclear magnetic resonance (13CNMR), carbon-hydrogen nitrogen sulfur (C-H-N-S), thermal analysis (TG), atomic-absorption-flame (AAF), conductivity and Magnetic susceptibility.

Examining new compounds through a calculation of photodegradation polystyrene films, assessed photo-stability activities. Results indicate Pt<sub>2</sub>L<sub>3</sub> > Pd<sub>2</sub>L<sub>3</sub> > Cu<sub>2</sub>L<sub>3</sub> > Ni<sub>2</sub>L<sub>3</sub> > Co<sub>2</sub>L<sub>3</sub> > L<sub>3</sub> > PS. Polymer stability is given for this the analysis of the reduction of weight, molecular average, reveals a more stable polystyrene PS.

**Keywords:** New Schiff base, Condensation reaction, Photo-stability, Photodegradation, New complexes

## Correspondence:

Ali M. A. Al – Khazraji

Department of Chemistry, College of Education for Pure Sciences, Ibn al – Haytham, University of Baghdad, Baghdad, Iraq

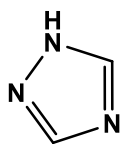
E-mail: [alimudher82@gmail.com](mailto:alimudher82@gmail.com)

DOI: [10.31838/srp.2020.5.71](https://doi.org/10.31838/srp.2020.5.71)

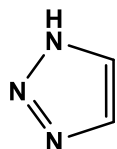
©Advanced Scientific Research. All rights reserved

## INTRODUCTION

Heterocyclic compounds are the main organic substrate class which contains a minimum of two different atom types in the ring [1-3]. The inorganic heterocyclic and ringed mixed rings without atoms are organic heterocyclics, as are heteroatoms and heteroatom as (N, O & S) [4]. More than half of all recognized chemicals have at least a heterocyclic phase, making them the largest class of organic compounds [5]. Heteroatom presence offers many physical and chemical properties of heterocyclic compounds. The heterocycles are common in nature and are of great importance for human life because many natural products such as vitamins, hormones, antibiotics, and pigments contain their structural units. This indicates that the concepts of biologically active molecules have gained significant interest. Heterocyclic nitrogen is a synthetic obstacle for a variety of natural products with physiological activity [6,7]. Triazole is a class of organic heterocyclic compounds, also known as pyrroldiazole. It comprises one class of five members of the diunsaturated ring structure consisting of three atoms, and two atoms of carbon at the non-adjacent site, Two triazole isomers [8-10]:

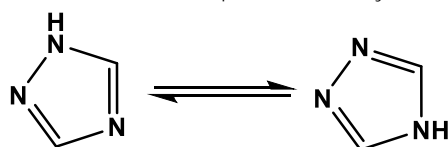


(1)



(2)

In two tautomeric forms, 1,2,4-triazoles exist. 1H and 4H-1,2,4- triazole are considered pharmaceutically essential [11]



The amine and the sulfur atom must be a perfect ligand of soft and hard nitrogen atoms. The terephthalaldehyde interacts with this ligand, which is a new Schiff base ligand. Also, the chemical processes and operation of this new Schiff base can be researched extensively via the coordination of Different metal ions [12-15]. Our analysis of metal transition complexes is continuously interested. The new ligand (Schiff base) and complexes are synthesized, characterized, and tested by the measurement of the polystyrene film for photodegradation of evaluating new compounds in a photo-stability operation.

## EXPERIMENTAL

### Materials and methods

Sigma-Aldrich obtained all the chemicals and solvents used.

#### 1- Synthesis of ethyl-4-chlorobenzoate (2)

Ethyl-4-chlorobenzoate was synthesized according to the present method scheme 1: 0.026 mmole of 4-chlorobenzoic acid (5 g) has been dis-solved in (40 ml) of EtOH (C<sub>2</sub>H<sub>5</sub>OH). Adding (4 ml) of H<sub>2</sub>SO<sub>4</sub> conc. to the reaction was acidic. The reaction mixture was then heated for 4 hours under reflux. The remaining alcohol has been distilled and is cooled with a 10 % sodium bicarbonate solution followed by a saturated solution of sodium chloride, to eliminate vacuum-filtered residual acid. The ethyl-4-chlorobenzoate crystal was eventually produced [16].

#### 2- Synthesis of 4-chlorobenzohydrizde (3)

4-chlorobenzohydrizde was synthesized according to the present method scheme 1: A total of (15 ml) of ethanol was used for dissolution of ethyl-4-chlorobenzoate (0.01, 1.76 gm). 80 % of (30 ml) hydrazine was added then heated and reflux 10 hours. A thin-layer chromatography (TLC) was used to track the reaction. The obtained solid was vacuum-dried and filtered. The obtained powder has a white crystal needle filled with ice-cold water [16].

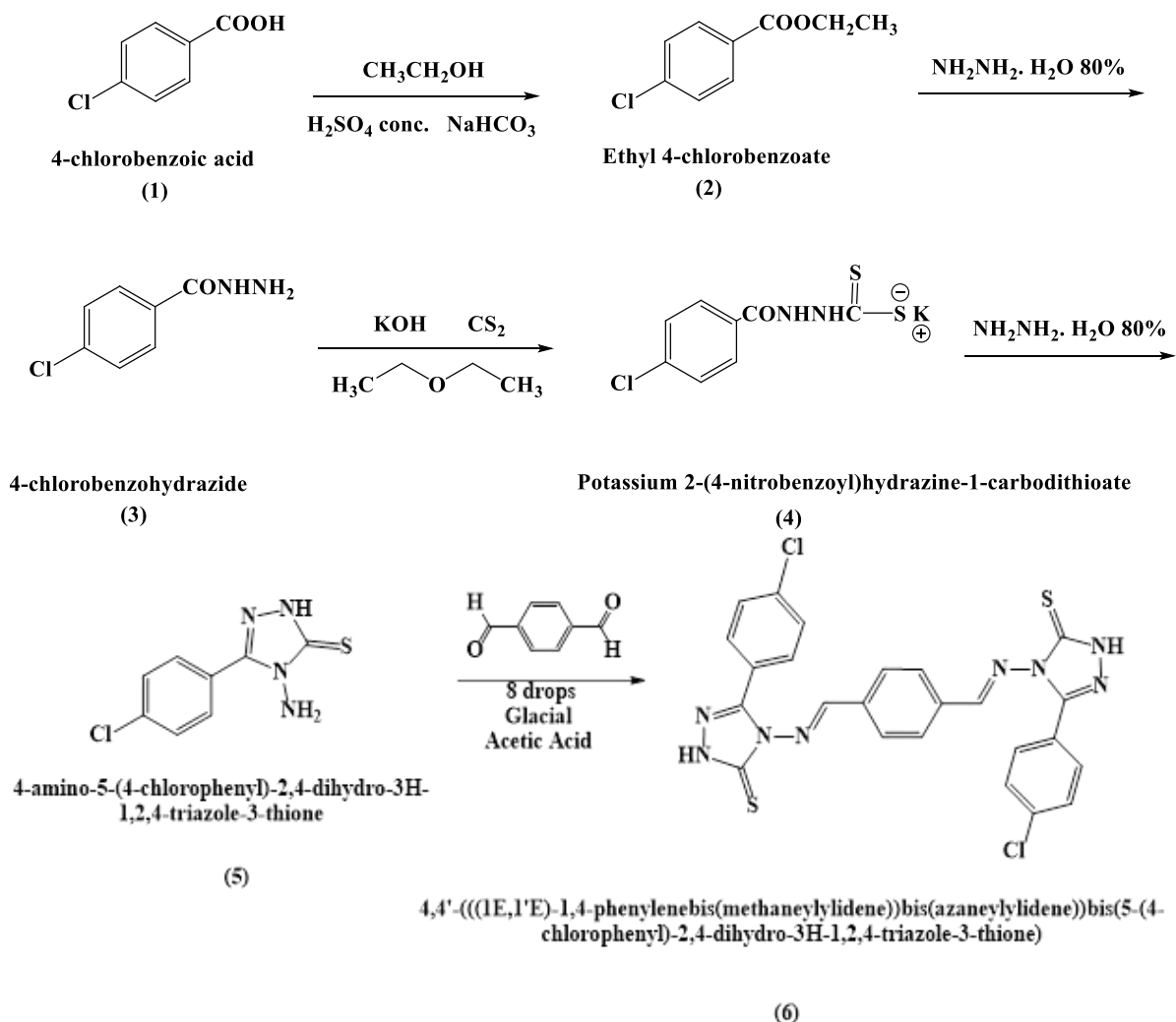
3- Synthesis of potassium-2- (4-chlorobenzoylhydrazine-1-carbodithio-ate) (4)  
 Potassium-2- (4- chlorobenzoylhydrazine-1-carbodithio-ate) was synthesized according to the present method scheme 1: KOH (0.0135 mmol) Potassium hydroxide has been dissolved in absolute ethanol (30 ml). 4-chlorobenzoylhydrazide were then combined with 0.0135 mmol of carbon-disulfide (CS<sub>2</sub>) in the mixture under stirring at room-temperature of 25 °C for (12 hours). Added (200 ml) diethyl ether to cool the reaction with stirred for 10 minutes. A filter was obtained to form solid, and the diethyl ether washed under vacuum.

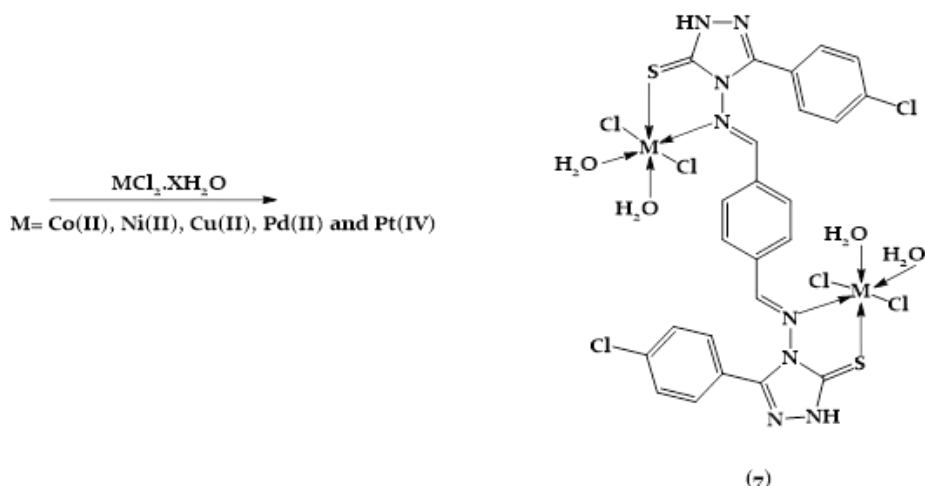
4- Synthesis of 4-amino-5-(4-chlorophenyl)-2, 4-dihydro-3H-1, 2, 4-triazole-3-thione (5)  
 4-amino-5-(4-chlorophenyl)-2, 4-dihydro-3H-1, 2, 4-triazole-3-thione was synthesized according to the present method scheme 1: A-compound (4) (0.009mmol) has been added slowly to (20 ml) of hydrazine Hydrate 80%. For six hours the mixture has refluxed. A color change is observed in the green reaction. Thin-layer chromatography (TLC) was used to monitor the reaction. Concentrated HCl (PH=3) acidified the contenting. The precipitation was applied to the compound under a vacuum.

5- Synthesis of ligand 4, 4'- ((( 1E, 1'E)-1,4-phenylenebis-(methane-ylidene))-bis-(azaneylylidene))-bis-(5-(4-chlorophenyl)-4H-1,2,4-triazole-3-thione) (6) (L<sub>3</sub>)

(L<sub>3</sub>) was synthesized according to the present method scheme 1: A (5) (0.009 mmol) compound was dissolved and aggravated in absolute ethanol (30 ml). Terephthalaldehyde has then been added (0.003 mmol). Added eight drops of Glacial acetic acid was acidic to the reaction. All mixture heated for 10 hours under reflux. Thin-layer chromatography (TLC) was used to monitor the reaction then filtered under vacuum to obtained powder [17,18].

6- Synthesis of transition metal complexes (7)  
 The transition metal Complexes of Co(II), Cu(II), Ni(II), Pt(II), and Pd(II) were synthesized from metallic salts of CoCl<sub>2</sub>.6H<sub>2</sub>O, CuCl<sub>2</sub>.2H<sub>2</sub>O, NiCl<sub>2</sub>.6H<sub>2</sub>O, H<sub>2</sub>PtCl<sub>6</sub>.6H<sub>2</sub>O and PdCl<sub>2</sub> with (L<sub>3</sub>), in (2: 1) As a ratio of metal to ligand according to the scheme 1. The final reaction had been heated for 4 hours under reflux. The precipitate was filtered and eventually washed from total ethanol by distilled water [19].





Scheme 1: new Schiff bases and their complexes, general synthetic path

## RESULT AND DISCUSSION

Table (1) show the information indicative of new ligand from Schiff base and their complexes by in (2: 1) As a ratio of metal to ligand, the ligands were burdened with metal,

C.H.N.S. analyzes and atomic absorption(AA) alongside the new ligand from Schiff base physical properties and their complexes were present. The DMSO was soluble in all complexes.

Table 1: New Schiff Base (L<sub>3</sub>) and its complexes ( physical properties and analytical data).

Symbol	Color	MP °C	Yield %	M.Wt	Micro Elemental Analysis Found (calc.)				Metal content % Found (calc.)	Chloride content % Found (calc.)
					C %	H %	N %	S %		
L	Dark orange	260	69	551.47	50.33 (50.29)	2.91 (2.79)	24.67 (24.45)	11.33 (11.17)	-----	-----
Co <sub>2</sub> L	Brown	274	61	928.86	33.78 (33.59)	3.36 (3.23)	12.24 (12.06)	7.06 (6.89)	12.81 (12.69)	-----
Ni <sub>2</sub> L	Brown	292 (dec.)	58	882.38	32.84 (32.64)	3.03 (2.72)	12.74 (12.69)	7.44 (7.25)	13.52 (13.30)	-----
Cu <sub>2</sub> L	Brown	205	63	892.1	32.43 (32.28)	2.81 (2.69)	12.71 (12.55)	7.29 (7.17)	14.33 (14.25)	-----
Pd <sub>2</sub> L	Dark orange	278	59	923.86	31.29 (31.17)	2.22 (1.95)	12.36 (12.12)	7.04 (6.93)	23.21 (23.04)	-----
Pt <sub>2</sub> L	Bright yellow	300< (dec.)	62	1267.14	22.93 (22.52)	1.61 (1.56)	11.13 (10.95)	5.17 (5.00)	30.23 (30.19)	-----

The FT-IR spectrum of new Schiff base L and their complexes

The FT-IR spectrum characterized a new schiff base ligand and its complexes Table (2), Figures (1-7). The result show absorption bands  $\nu$ : 3278  $\text{cm}^{-1}$  (NH), 3102  $\text{cm}^{-1}$  (C-H) ar., 2753  $\text{cm}^{-1}$  (S-H), 1694  $\text{cm}^{-1}$  (CH=N) azo-methane, 1600  $\text{cm}^{-1}$  (C=C) and 1419  $\text{cm}^{-1}$  (C=S) for the ligand [20,21]. In  $\nu$ ,

1691  $\text{cm}^{-1}$  (CH=N) azo-methane [20], 1433  $\text{cm}^{-1}$  (C=S), while the complexes exhibited bands. The band intensity shifting for ligand (L<sub>3</sub>) attributed to the Ligand-Metal coordinate [22]. The new (Metal-N) and (Metal-S) bands and (Metal-Cl) bands at (200-590  $\text{cm}^{-1}$ ) are also apparent [23].

Table 2: FT-IR data of new Schiff base ligand and their complexes

Symbol	$\nu(\text{C=N})$	$\nu(\text{C=S})$	$\nu(\text{M-N})$	$\nu(\text{M-S})$	$\nu(\text{M-Cl})$
L	1693	1425	-----	-----	-----
Co <sub>2</sub> L	1660	1423	540	468	310
Ni <sub>2</sub> L	1695	1425	543	468	320
Cu <sub>2</sub> L	1701	1423	540	464	337
Pd <sub>2</sub> L	1695	1429	540	466	312
Pt <sub>2</sub> L	1697	1429	557	451	300

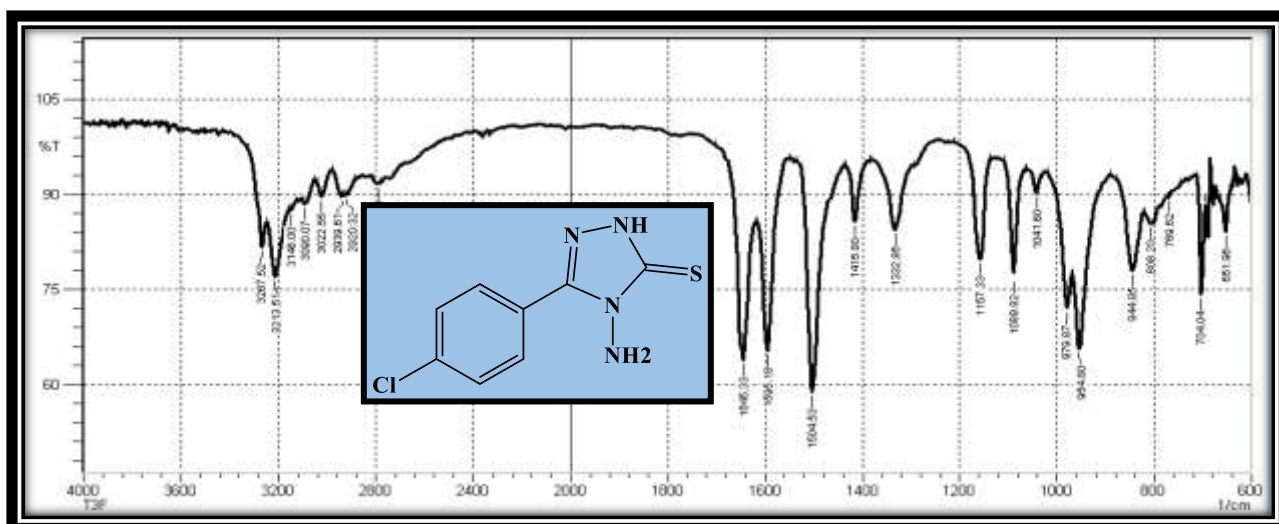


Figure 1: FT-IR spectrum of 4-amino-5-(4-chlorophenyl)-2,4-dihydro-3H-1,2,4-triazole-3-thione

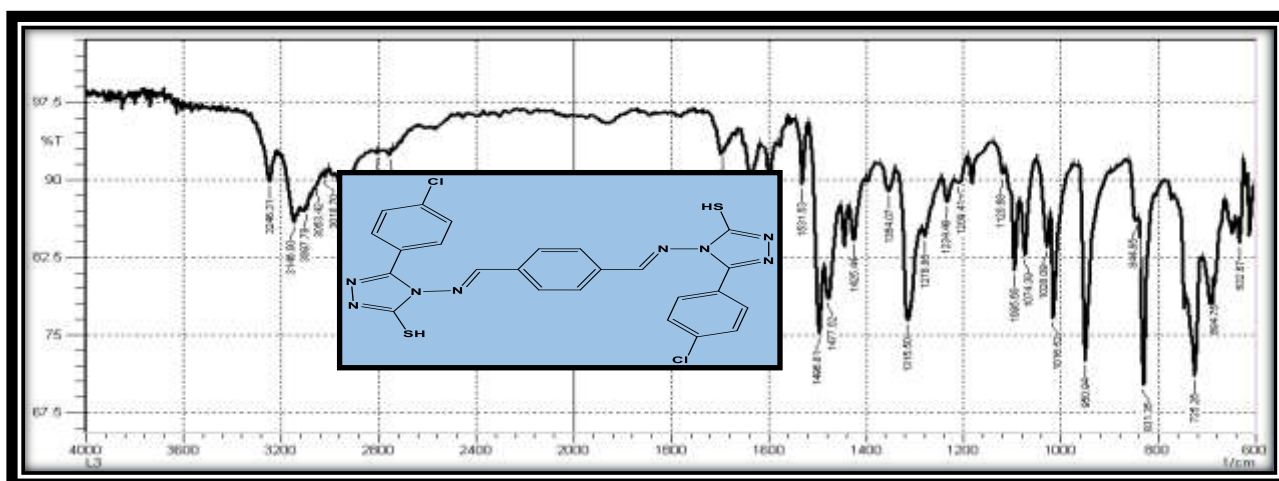


Figure 2: FT-IR spectrum of (L<sub>3</sub>) 4,4'-(((1E,1'E)-1,4-phenylene-bis(methanylylidene))-bis(azanylylidene))-bis-(5-(4-chlorophenyl)-4H-1,2,4-triazole-3-thione)



Figure 3: FT-IR spectrum of (Co<sub>2</sub>L<sub>3</sub>) complex



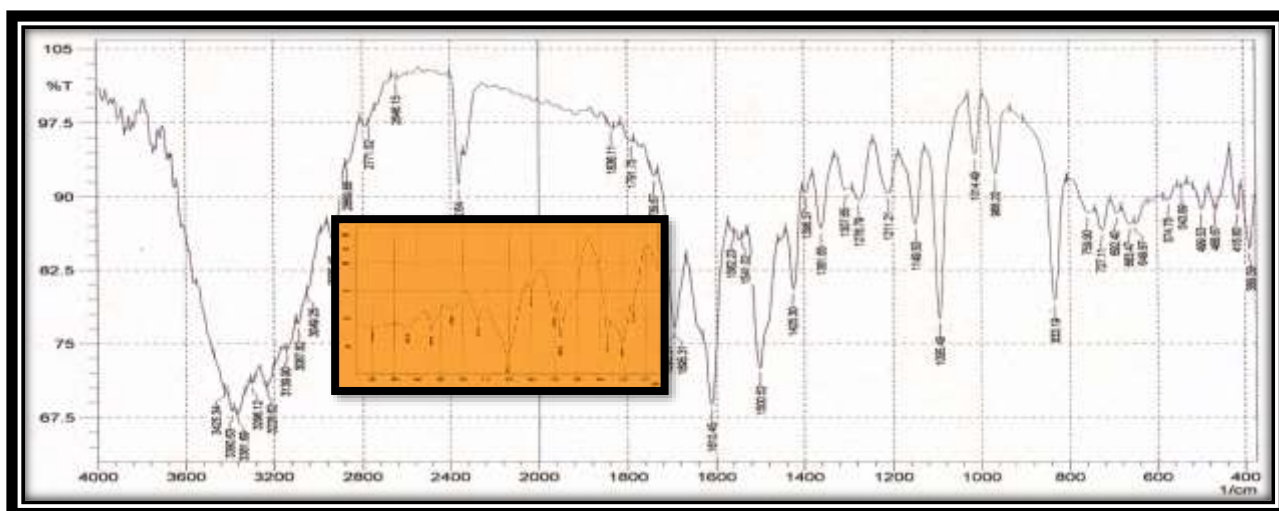


Figure 4: FT-IR Spectrum of (Ni<sub>2</sub>L<sub>3</sub>) Complex

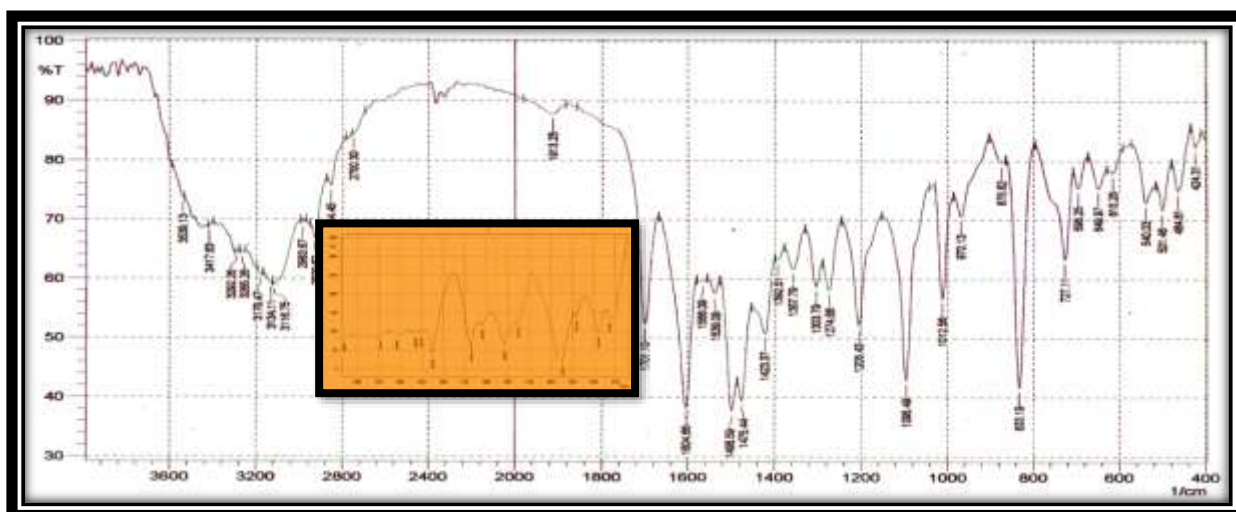


Figure 5: FT-IR Spectrum of (Cu<sub>2</sub>L<sub>3</sub>) Complex

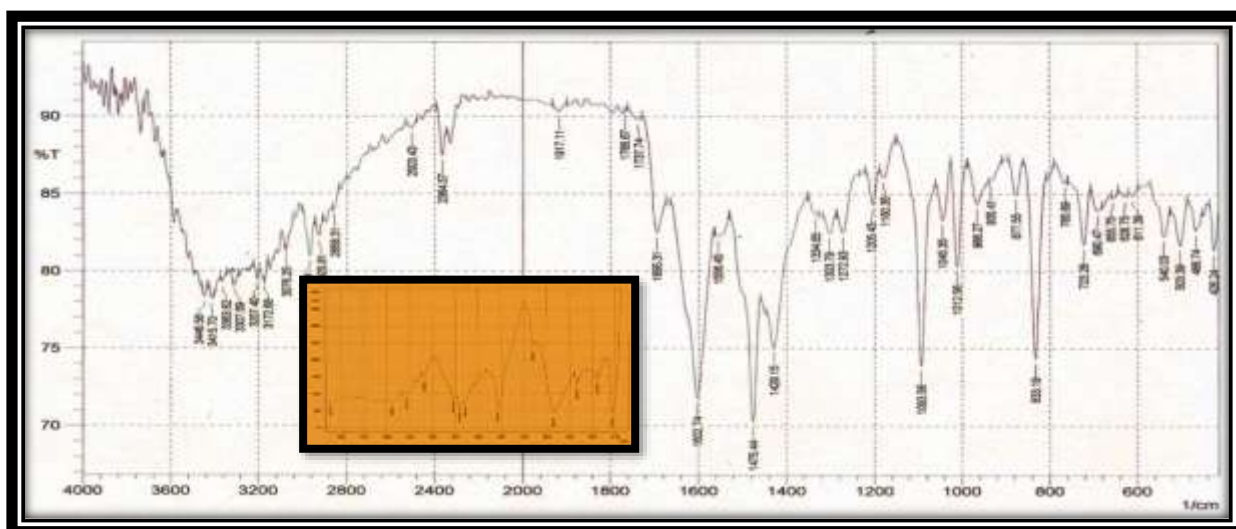


Figure 6: FT-IR Spectrum of (Pd<sub>2</sub>L<sub>3</sub>) Complex

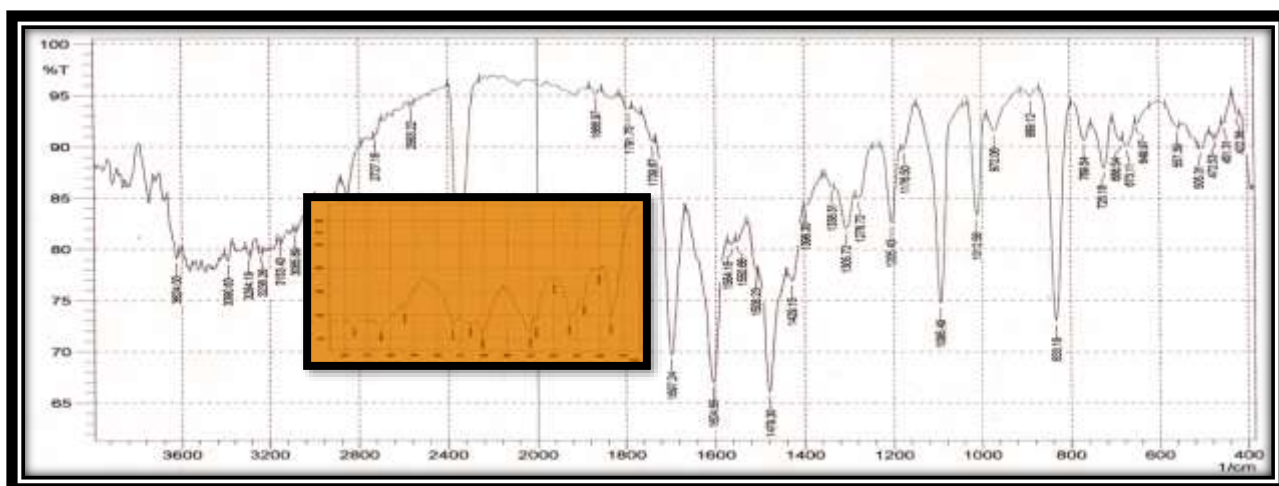


Figure 7: FT-IR Spectrum of (Pt<sub>2</sub>L<sub>3</sub>) Complex

<sup>1</sup>H-NMR and <sup>13</sup>C-NMR spectrum of synthesized (L<sub>3</sub>)  
<sup>1</sup>H-NMR spectrum of (L<sub>3</sub>) shown in Figure (8-9), the signals at (δ, ppm): 14.01 (1H, s, SH) [24], 9.94 (1H, s, CH=N), 8.19 (4H, m, CH ar.), while the <sup>13</sup>C-NMR shown in Figure (10-

11), signals at (δ, ppm): 148 (C- 1, 2, 4- triazole-ring), 157 (CH=N) (C azo-methane), 135 (C-Cl) group, 160 (C=S) thione group.

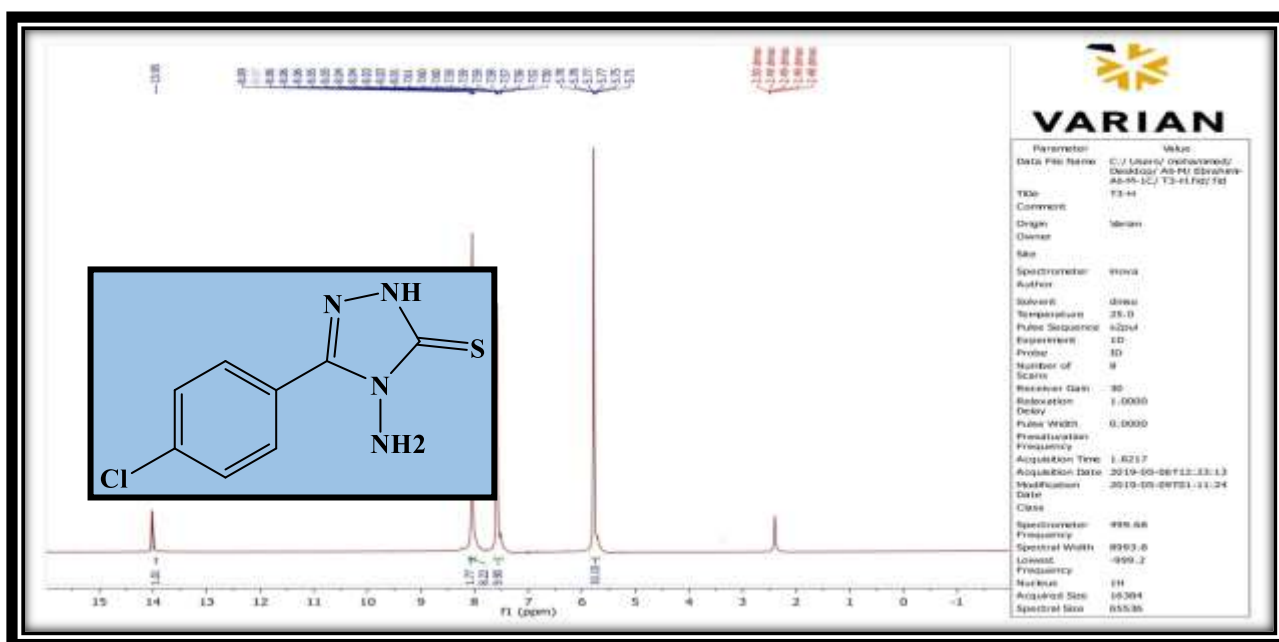


Figure 8: <sup>1</sup>H-NMR spectrum for 4-amino-5-(4-chlorophenyl)-2,4-dihydro-3H-1,2,4-triazole-3-thione

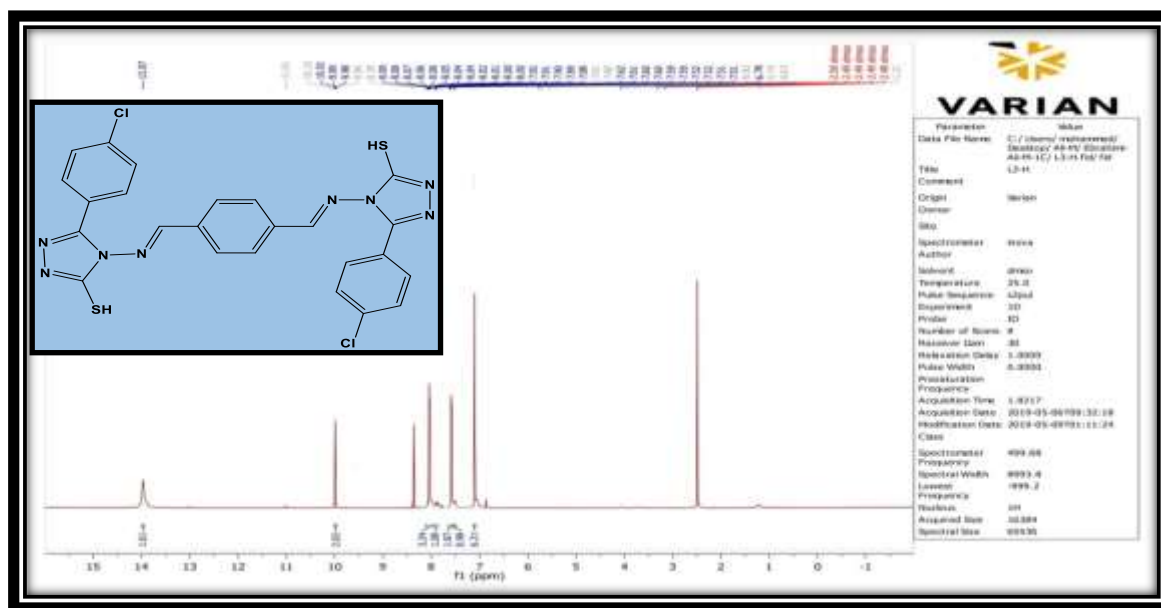


Figure 9: <sup>1</sup>H-NMR spectrum for (L<sub>3</sub>) 4, 4'-(((1E, 1'E)-1,4-phenylene-bis(methane-ylidene))-bis-(azane-ylidene))-bis-(5-(4-chlorophenyl)-4H-1,2,4-triazole-3-thione)

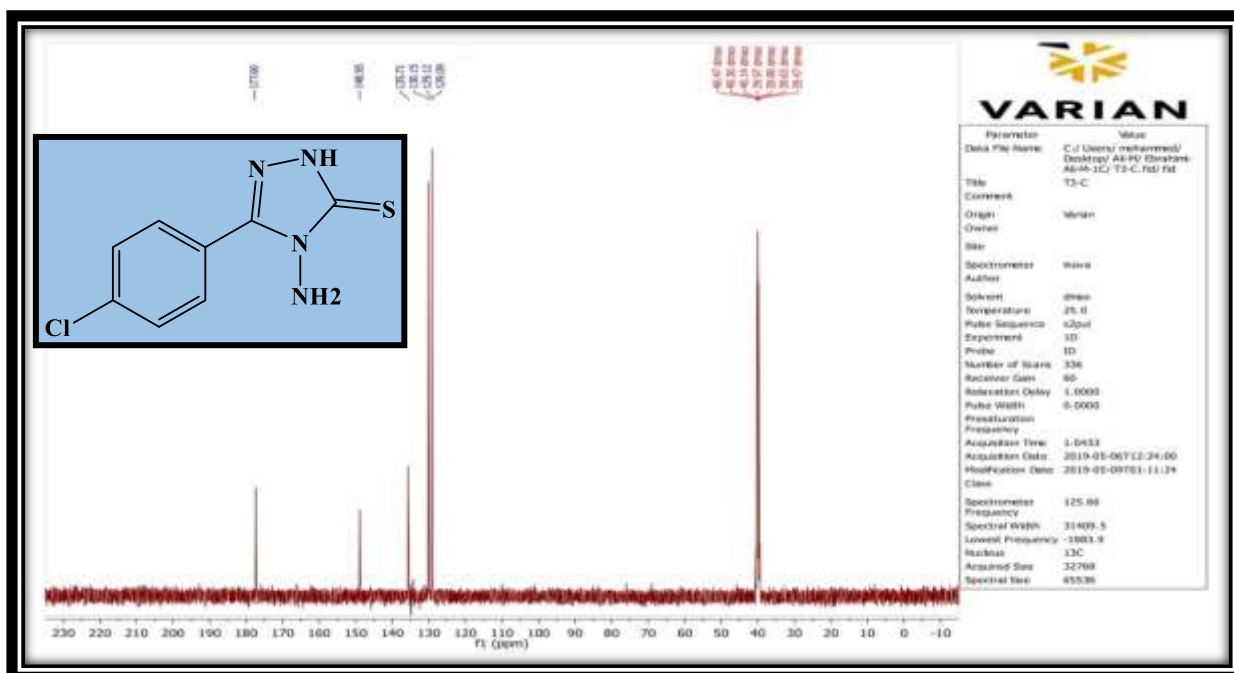


Figure 10: <sup>13</sup>C-NMR spectrum for 4-amino-5-(4-chlorophenyl)-2,4-dihydro-3H-1,2,4-triazole-3-thione

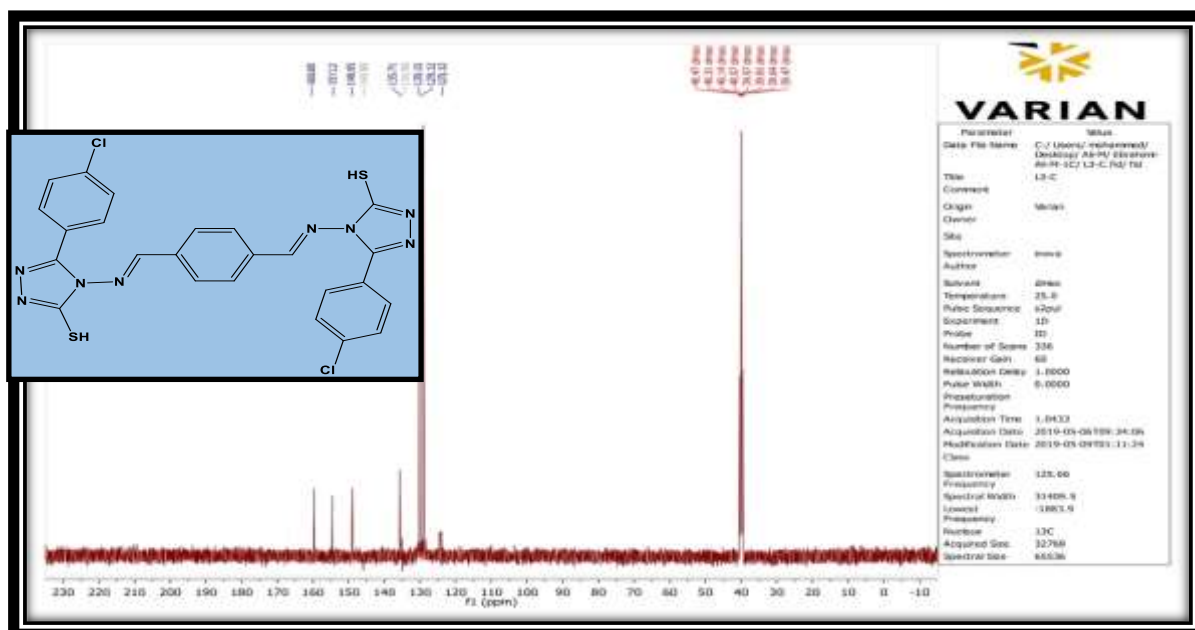


Figure 11:  $^{13}\text{C}$ -NMR spectrum for ( $\text{L}_3$ ) 4, 4'-(((1E, 1'E)-1,4- phenylene-bis-(methane-ylidene))-bis-(azane-ylidene))-bis-(5-(4-chlorophenyl)- 4H-1,2,4-triazole-3-thione)

Also, magnetic sensitivity and molar conduction are summarized in table 3.

Table 3: Molar conductivity and metal-complexes magnet susceptibility

Compound	Molar conductivity $\text{Ohm}^{-1} \text{cm}^2 \text{mole}^{-1}$	Magnetic susceptibility (B.M)	
		Cal.	Found
$\text{Co}^2\text{L}$	13.43	4.01	4.15
$\text{Ni}^2\text{L}$	9.98	2.78	2.88
$\text{Cu}^2\text{L}$	17.42	1.73	1.77
$\text{Pd}^2\text{L}$	15.83	0.03	0.01
$\text{Pt}^2\text{L}$	18.74	0.07	0.09

Electronic spectra (Uv.vis) of new Schiff base ( $\text{L}_3$ )

Three bands of absorption (238 nm,  $42016 \text{ cm}^{-1}$ ), (350 nm,  $28571 \text{ cm}^{-1}$ ), allocation to ( $\pi \rightarrow \pi^*$ ), ( $n \rightarrow \pi^*$ ) intra-light transitions, and (411 nm,  $24330 \text{ cm}^{-1}$ ) intake allo-cated to ( $n \rightarrow \pi^*$ ).

Electronic-spectrum (Uv.vis) of Cobalt-(II) complex

two bands of absorption at (650 nm,  $15385 \text{ cm}^{-1}$ ) and (538 nm,  $18587 \text{ cm}^{-1}$ ) were observed for the electronics spectrum ( $\text{Co}_2\text{L}_3$ ) complex., That could be related to the transition [ $^4\text{T}_{1g} \rightarrow ^4\text{A}_{2g}$ ] (F) ( $\nu_2$ ) and [ $^4\text{T}_{1g} \rightarrow ^4\text{T}_{1g}$ ] (P) ( $\nu_3$ ) respectively, Octahedral geometry these clicks. Based on this assignment ( $\nu_1$ ) for  $d^7$  of the diagram (Tanabe-sugarano) was calculated, the Estimated value of ( $\nu_1$ ) by transition  $^4\text{T}_{1g} \rightarrow ^4\text{T}_{2g}$  (F) to ( $7938 \text{ cm}^{-1}$ ). In addition to the 10 Dq, B, and  $\beta$  ( $\text{Co}_2\text{L}_3$ ) values, respectively, it is (75550, 458, and 0,69). The sensitivity of the magnet and molar conductivity measurement suggested that the complex is (4.15) B.M.

Electronic-spectrum (Uv.vis) of Nickel-(II) complex

There are two ( $698 \text{ nm}$ ,  $14327 \text{ cm}^{-1}$ ) and ( $460 \text{ nm}$ ,  $21739 \text{ cm}^{-1}$ ) transitions, respectively, of [ $^3\text{A}_{2g} \rightarrow ^3\text{T}_{1g}$ ] (F) ( $\nu_2$ ) and [ $^3\text{A}_{2g} \rightarrow ^3\text{T}_{1g}$ ] (P) ( $\nu_3$ ), respectively. Transformations of the ( $\text{Ni}_2\text{L}_3$ ) complex are shown as the electronic spectrum. The bands show a Ni (II) ion octahedral geometry. Transition [ $^3\text{A}_{2g} \rightarrow ^3\text{T}_{2g}$ ] (F) can be attributed to ( $\nu_1$ ) to ( $11677 \text{ cm}^{-1}$ ). The magnetism value (2.88) B.M coincides with the octahedral configuration of Ni ( II) ions, while the nonionic characterization of these structures results in conductance calculation.

Electronic-spectrum (Uv.vis) of copper-(II) complex

The chloroform complex electronics spectrum (Uv.vis) of ( $\text{Cu}_2\text{L}_3$ ) tends to be low energy in a shallow band of  $14285 \text{ cm}^{-1}$  and high strength of [ $^2\text{E}_g \rightarrow ^2\text{T}_{2g}$ ] and [ $\text{L} \rightarrow \text{Cu}$ ] (C.T) respectively. ( $\text{Cu}_2\text{L}_3$ ) magnetism-moment (1.77) B.M is respectively, and the calculation of non-electoral cond-



activity. The Cu (II) data indicate that the complex octahedral (Cu<sub>2</sub>L<sub>3</sub>) exists.

Electronic-spectrum (Uv.vis) of palladium-(II) Complex Three bands of absorption at (472 nm, 21186 cm<sup>-1</sup>), (390 nm, 25641 cm<sup>-1</sup>) and (340nm, 29412 cm<sup>-1</sup>) for the spectrum of light brown (Pd<sub>2</sub>L<sub>3</sub>), each with the product of [<sup>1</sup>A<sub>1g</sub>→<sup>1</sup>B<sub>1g</sub>], [<sup>1</sup>A<sub>1g</sub>→<sup>1</sup>E<sub>1g</sub>] and [L → Pd] (C.T) respectively. Such strips' locations conform well to the geometry of tick square planers. However, the magnetism moment value for this complex is (0.01) B.M while the calculation of the behavior of these complexes ticks the non-ionic moment.

Electronic-spectrum (Uv.vis) of platinum-(IV) complex The electronic spectrum (UV.Vis) of (Pt<sub>2</sub>L<sub>3</sub>) was assigned to [<sup>1</sup>A<sub>1g</sub> → <sup>3</sup>T<sub>1g</sub>], [<sup>1</sup>A<sub>1g</sub> → <sup>3</sup>T<sub>2g</sub> ] and [L → Pt ] (C.T) respectively, at the ranges (508 nm, 19685 cm<sup>-1</sup>), (460 nm, 21739 cm<sup>-1</sup>), and (410 nm, 24390 cm<sup>-1</sup>). The current (Pt<sub>2</sub>L<sub>3</sub>) (d<sup>6</sup>) complex structure (0.24) B.M agrees with the octahedral structure around Pt (IV) is the magnetism moment value. According to the existence of such complexes, the cond-uctance test ticks the non-ionic.

Thermal-analysis (TG ) of the (L<sub>3</sub>) (new Schiff base ) and their complexes TG and DTA [25] compound thermal tests were applied in Table (4) at a heating range of nitrogen gas (N<sub>2</sub>) (25 -800) °C temperature heat (10 °C / min) and in the figure. (12-17).

Table 4: New Schiff base ligand and its complexes thermal decomposition data

Compound	Molecular Formula M.Wt	Step	Temp. range of the decomposition (TG) °C	Suggested Formula of loss	Mass loss %	
					Cal.	Found
L	C <sub>24</sub> H <sub>16</sub> Cl <sub>2</sub> N <sub>8</sub> S <sub>2</sub> 550.03	1	0 – 221	Cl	6.45	6.07
		2	221 – 352	2C <sub>6</sub> H <sub>4</sub> , 2CH	32.36	32.74
		3	352 – 595	C <sub>6</sub> H <sub>6</sub> , 2C <sub>2</sub> N <sub>3</sub> H	38.9	39.77
Co <sup>2</sup> L	C <sub>26</sub> H <sub>30</sub> Co <sub>2</sub> Cl <sub>6</sub> N <sub>8</sub> S <sub>2</sub> O <sub>5</sub> 928.86	1	0 – 162	H <sub>2</sub> O, EtOH	6.89	6.97
		2	162 – 354	2C <sub>6</sub> H <sub>4</sub> , 2CH, 3Cl	30.62	31.22
		3	354 – 595		28.79	27.71
Ni <sup>2</sup> L	C <sub>24</sub> H <sub>24</sub> Ni <sub>2</sub> Cl <sub>6</sub> N <sub>8</sub> S <sub>2</sub> O <sub>4</sub> 882.38	1	0 – 267	C <sub>6</sub> H <sub>4</sub> , 2CH, 2Cl	19.60	19.48
		2	267 – 411	2C <sub>6</sub> H <sub>4</sub>	17.22	17.42
		3	411 – 595	3Cl, 4H <sub>2</sub> O	20.22	21.34
Cu <sup>2</sup> L	C <sub>24</sub> H <sub>24</sub> Cu <sub>2</sub> Cl <sub>6</sub> N <sub>8</sub> S <sub>2</sub> O <sub>4</sub> 892.1	1	0 – 295	C <sub>6</sub> H <sub>4</sub> , 2CH, Cl	15.44	17.21
		2	295 – 378	C <sub>6</sub> H <sub>4</sub> , Cl	12.49	11.31
		3	378 – 595	C <sub>6</sub> H <sub>4</sub> , 2Cl	16.47	17.20
Pd <sup>2</sup> L	C <sub>24</sub> H <sub>18</sub> Pd <sub>2</sub> Cl <sub>6</sub> N <sub>8</sub> S <sub>2</sub> O 923.86	1	0 – 290	2C <sub>6</sub> H <sub>4</sub> , 2CH, Cl, H <sub>2</sub> O	25.05	23.23
		2	290 – 410	C <sub>6</sub> H <sub>4</sub> , C <sub>2</sub> N <sub>3</sub> H, Cl	19.53	17.70
		3	410 – 594	C <sub>2</sub> N <sub>3</sub> , 4Cl	22.83	21.92
Pt <sup>2</sup> L	C <sub>26</sub> H <sub>22</sub> Pt <sub>2</sub> Cl <sub>10</sub> N <sub>8</sub> S <sub>2</sub> O 1271	1	0 – 160	- OH	1.33	1.48
		2	160 – 330	- CH <sub>2</sub> CH <sub>3</sub> , C <sub>6</sub> H <sub>4</sub> , 2CH, 2Cl	15.81	16.70
		3	330 – 594	2C <sub>6</sub> H <sub>4</sub> , 6Cl	28.71	27.07

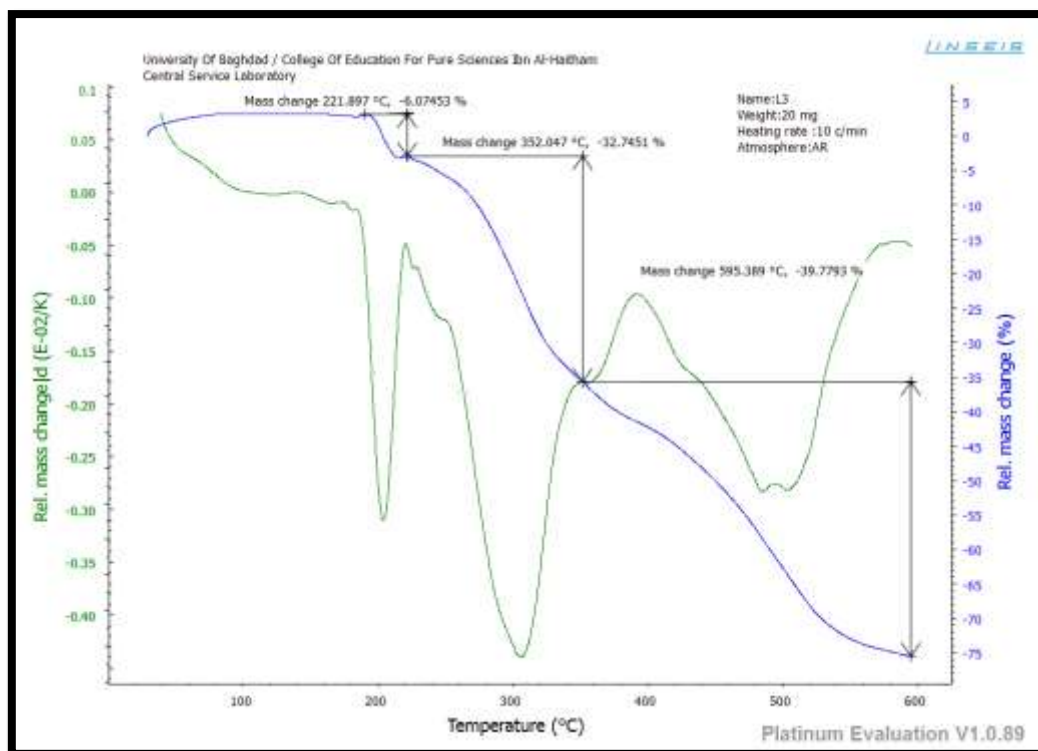


Figure 12: Thermo-graphs (TGA and DTA) of Ligand (L<sub>3</sub>)

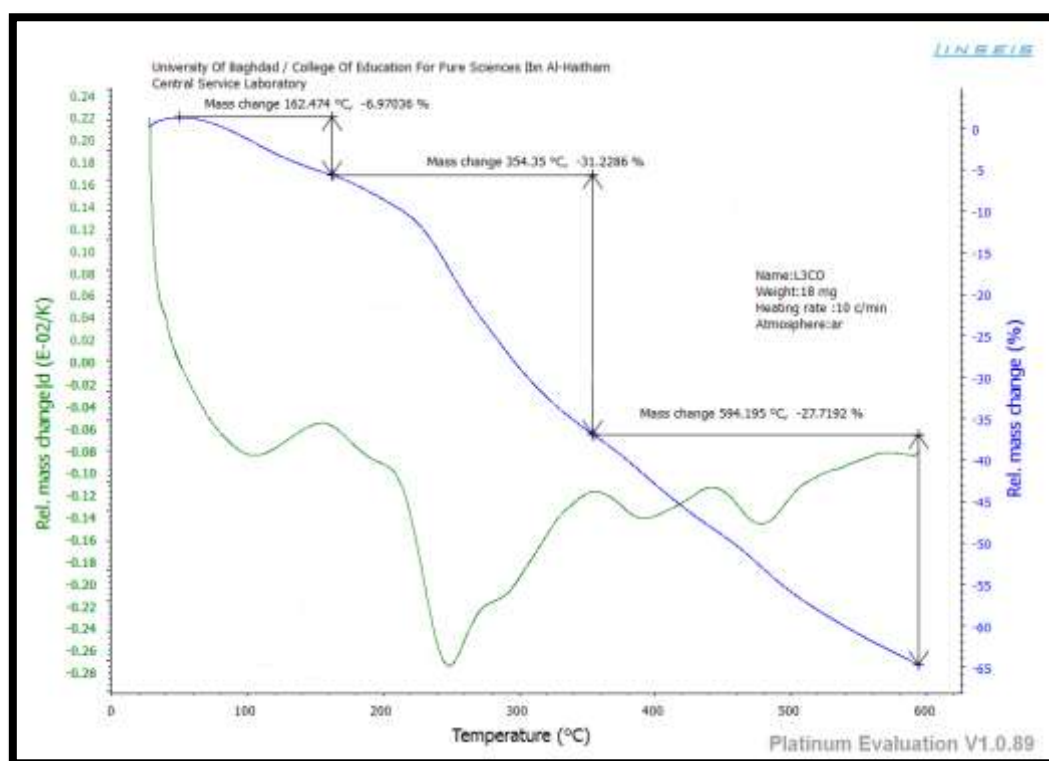


Figure 13: Thermo-graphs (TGA and DTA) of complex (Co<sub>2</sub>L<sub>3</sub>)

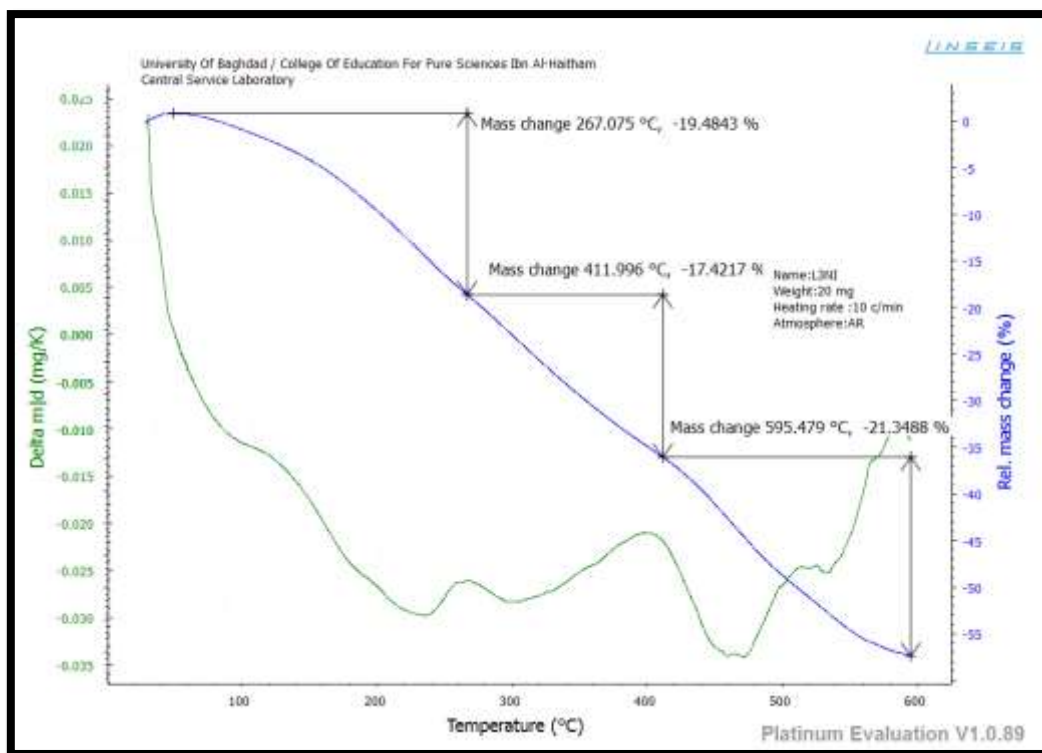


Figure 14: Thermo-graphs (TGA and DTA) of complex ( $Ni_2L_3$ )

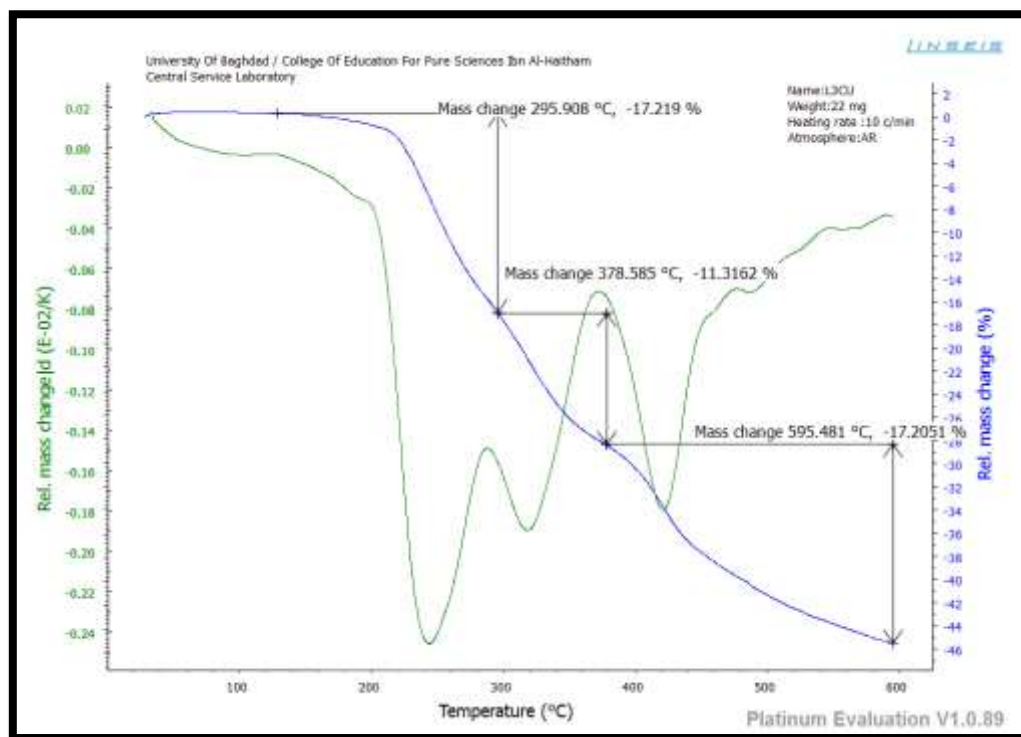


Figure 15: Thermo-graphs (TGA and DTA) of complex ( $Cu_2L_3$ )

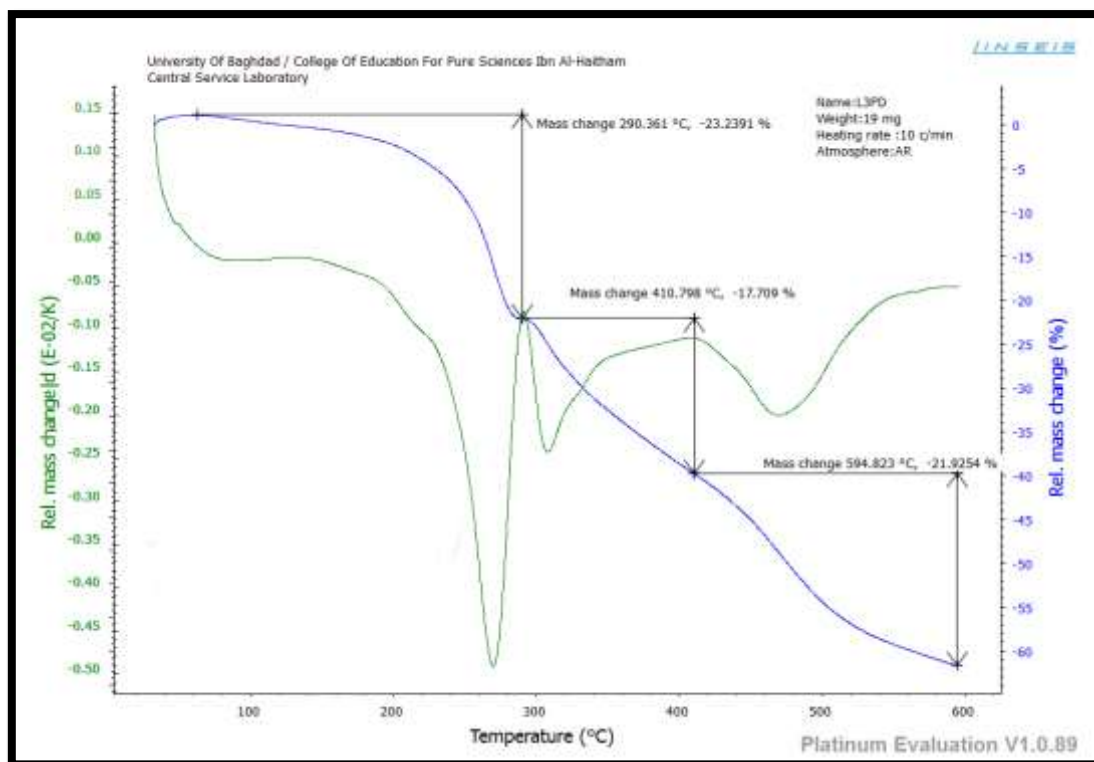


Figure 16: Thermo-graphs (TGA and DTA) of complex (Pd<sub>2</sub>L<sub>3</sub>)

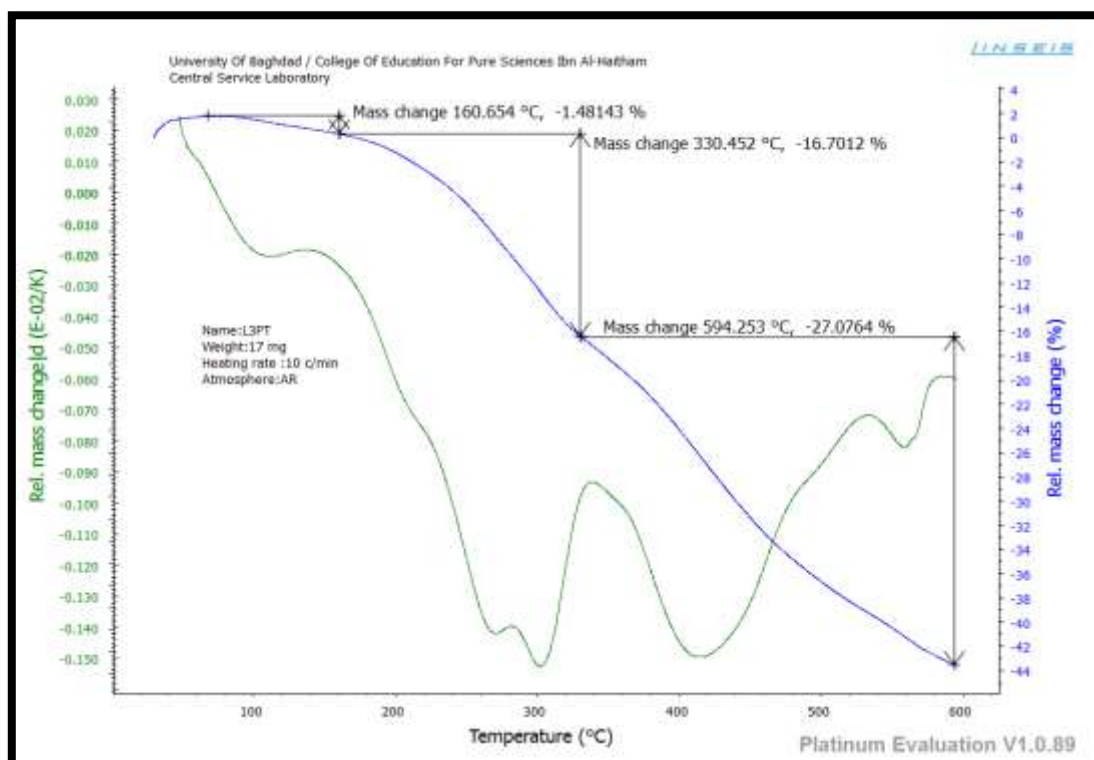


Figure 17: Thermo-graphs (TGA and DTA) of complex (Pt<sub>2</sub>L<sub>3</sub>)

#### Photo-stability

Polystyrene was used as a film to tested photostability in five metal complexes Cu(II), Co(II), Ni(II), Pd(II) and Pt(IV) with 4, 4'-(((1E, 1'E)-1, 4-phenylene-bis-(methanelylidene))-bis(azane-ylidene))-bis(5-(4-chlorophenyl) -

4H-1, 2, 4-triazole-3-thione) (L<sub>3</sub>). Specifically, the FT-IR spectrum shows the strength band is weakened by the radiation due to oxidation growth; in the formation of hydroxyl group it is due to large-band occurrences in the 3600–3200 cm<sup>-1</sup> band (see figure 20).

Figures (18-19) showing an exposure ray rate of ( $I_{CO}$ ) and ( $I_{OH}$ ) Indices increased by the sensitivity raying duration relative to Polystyrene without addition, showing Cu(II),

Co(II), Ni(II), Pd(II) and Pt(IV) metals. The most efficient photo stabilizes were observed with Pt (IV).

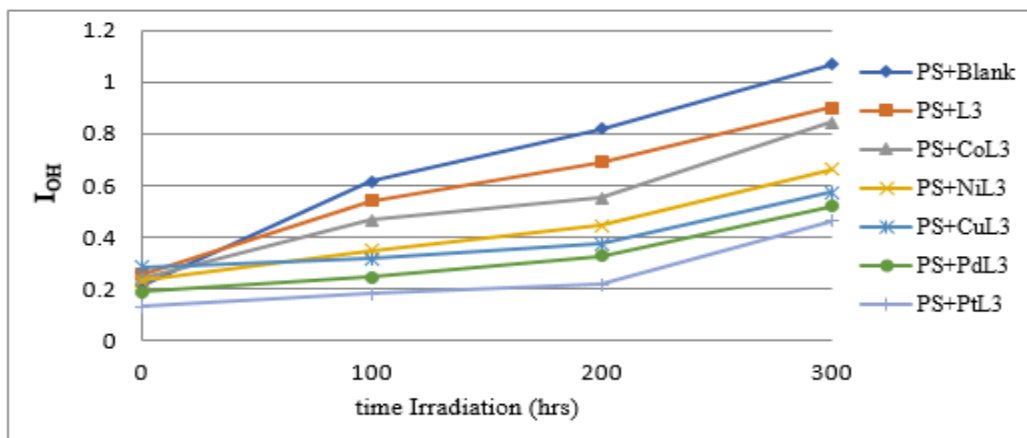


Figure 18:  $I_{OH}$  hydroxy index versus polystyrene film time irradiation ( $40 \mu\text{m}$ ) ( $0.5 \text{ W / v}$ ) additional

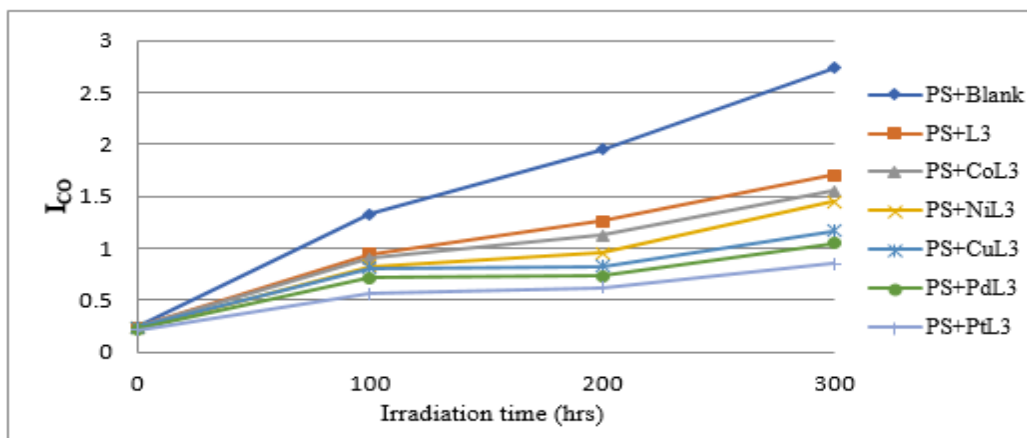


Figure 19:  $I_{CO}$  carbonyl index versus polystyrene film ( $40 \mu\text{m}$ ) time irradiation extra ( $0.5 \text{ w / v}$ ) additional

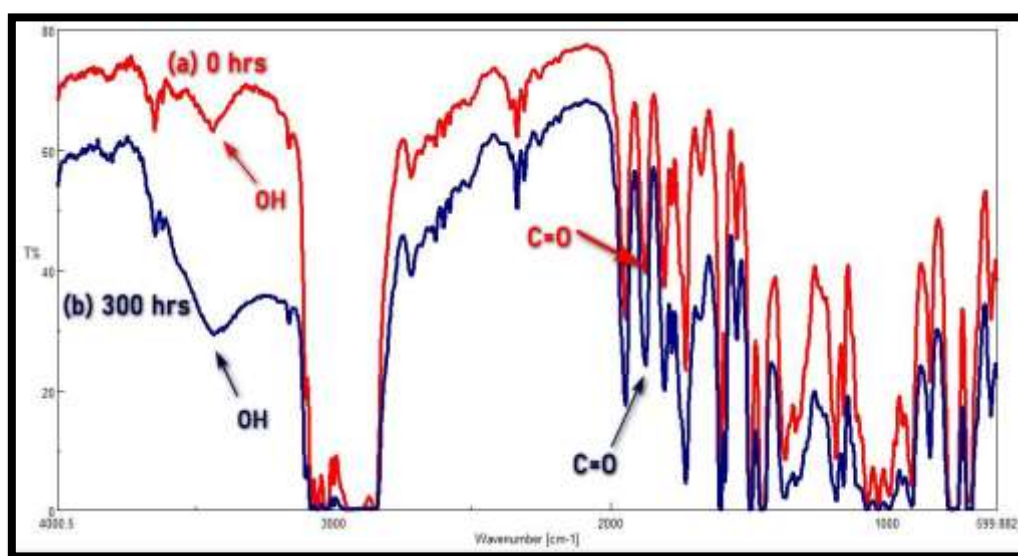


Figure 20: FT-IR polystyrene film spectrum (a) before and (b) after 300 hours of irradiation

Limit the adequacy of the weight loss stabilization process



Figure (21) shows the highest stability efficacy Pt(IV) due to decreased weight loss in order PS > L<sub>3</sub> > Co<sub>2</sub>L<sub>3</sub> > Ni<sub>2</sub>L<sub>3</sub> > Cu<sub>2</sub>L<sub>3</sub> > Pd<sub>2</sub>L<sub>3</sub> > Pt<sub>2</sub>L<sub>3</sub>

Polystyrene Film Degradation, Molecular Weight Reduction, and Volatilization (M.wt) from Loss of Weight. [26,27].

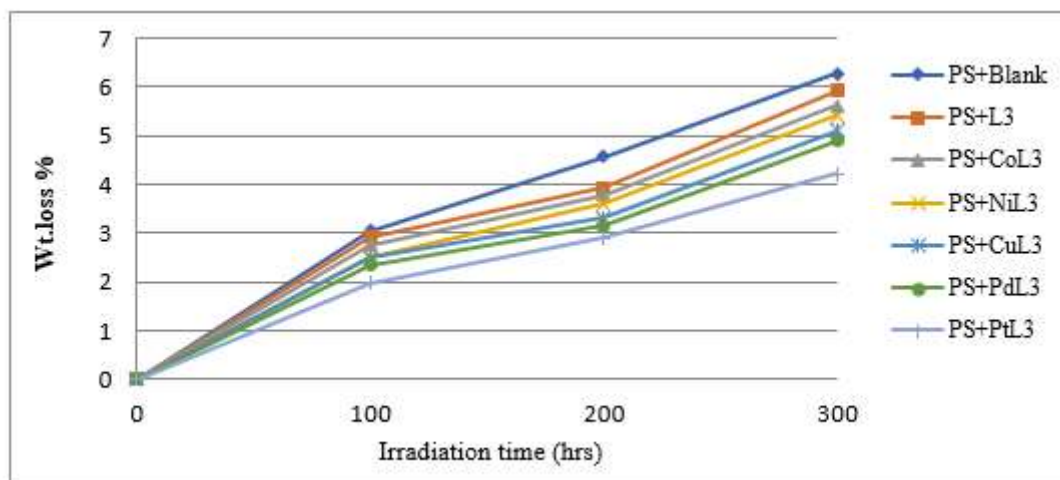


Figure 21: Extra thickness (0.5 w / v) loss of irradiation weight for PS films (40µm)

Molecular weight during photolysis variations of polystyrene films

Figure (22) indicates that polystyrene degradation contributed to a lower level of polystyrene and indicates a rapid initial decline in Mv due to a large chain break at a separate location in the polystyrene chain. Mv plot against exposure demonstrates additional time of film (0,5% w / v)

irradiation [28][29]. The total number of chain scissors using S (Eq. 8) where

Mv,0 = mean of M.wt viscosity at experiment start.

Mv,t = M.wt average irradiation-time viscosity.

$$S = Mv,0 / Mv,t - 1 \quad (8)$$

Table (5) show the variation of (Mv) extra thick-ness (0.5 w / v) with time (PS) (40 µm) film irradiation

Table 5: Distinction of (Mv) extra thick-ness (0.5 w / v) with time (PS) (40 µm) film irradiation

Compound	Irradiation time (hrs.)			
	0	100	200	300
PS+Blank	278439	233169	169218	93192
PS+L3	293861	244517	181139	102866
PS+CoL3	305422	263120	201389	133821
PS+NiL3	310791	278430	217160	137778
PS+CuL3	314933	281501	238710	144930
PS+PdL3	322575	290144	247114	168900
PS+PtL3	328116	299173	253319	178663

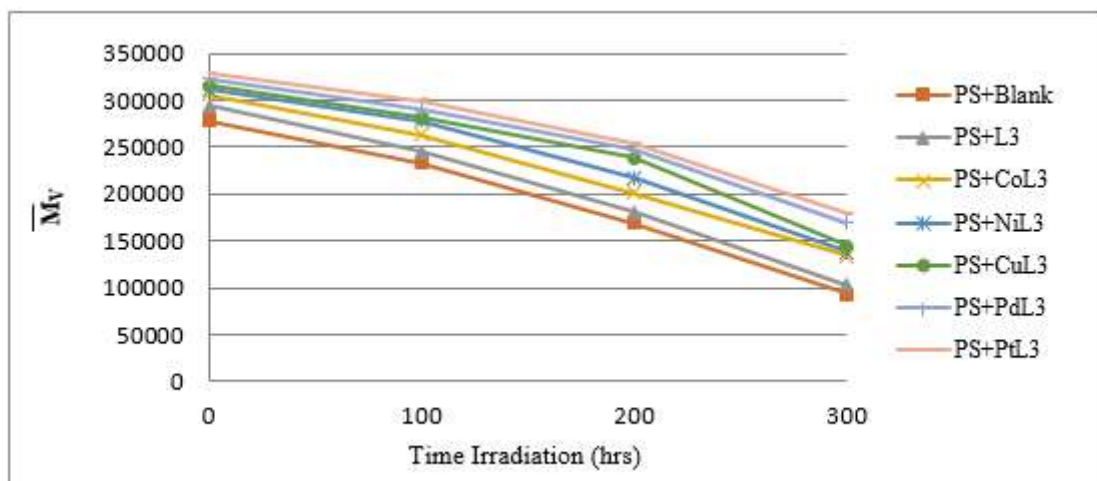


Figure 22: Mean viscosity difference M.wt-Mv with increased irradiated time for PS films (40µm) with an extra thickness (0.5w / v)

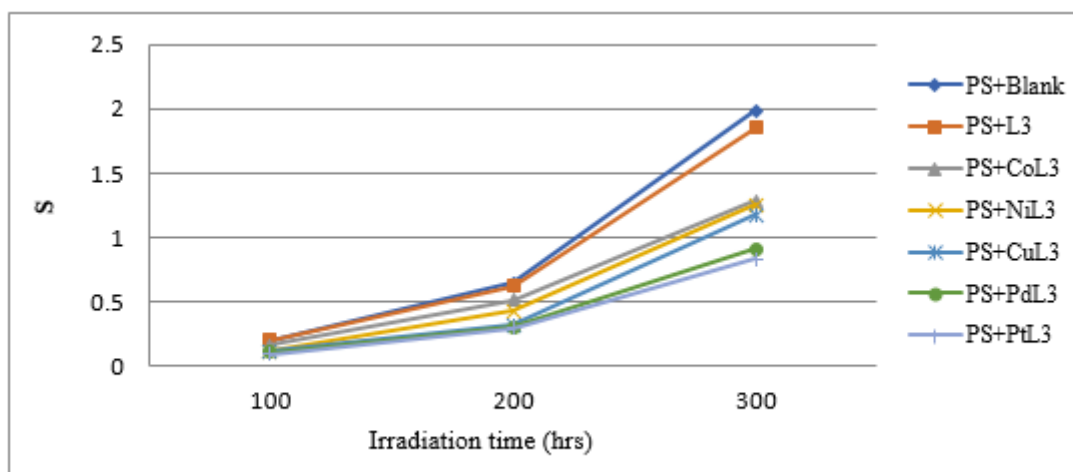


Figure 23: Distinction from central split (S) chain with extra thickness (0.5 W / v) times PS (40µm) film irradiation

The level of branching indicates an increase from data since cross-link can calculate the level of retrogradation ( $\alpha$ ) via (Eq. 9) are:

$$m = \text{Primitive of M.wt.} \\ \alpha = m \times S / Mv \quad (9)$$

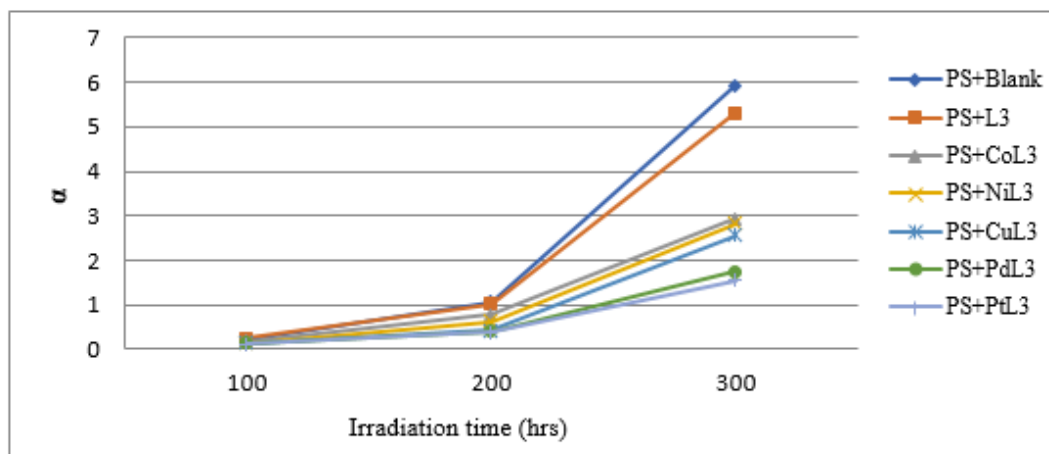


Figure 24: Value ( $\alpha$ ) disparity for the time radiation of (PS) (40µm) film (0.5 w / v) additional thickness

The degree of retrograde rate ( $\alpha$ ) versus the time of radiation as illustrated in Figure (25), the primary phases of polystyrene,  $\alpha$  grade assembly (DP)[30] and the number of

polystyrene monomeric unit (Eq.10) showing the degree of irradiation;

$M_0$  = the molecular-weight Mwt. of Monomer.

$M_n$  = the molecular-weight Mwt. average number

$$DP_n = X_n = M_n / M_0 \quad (10)$$

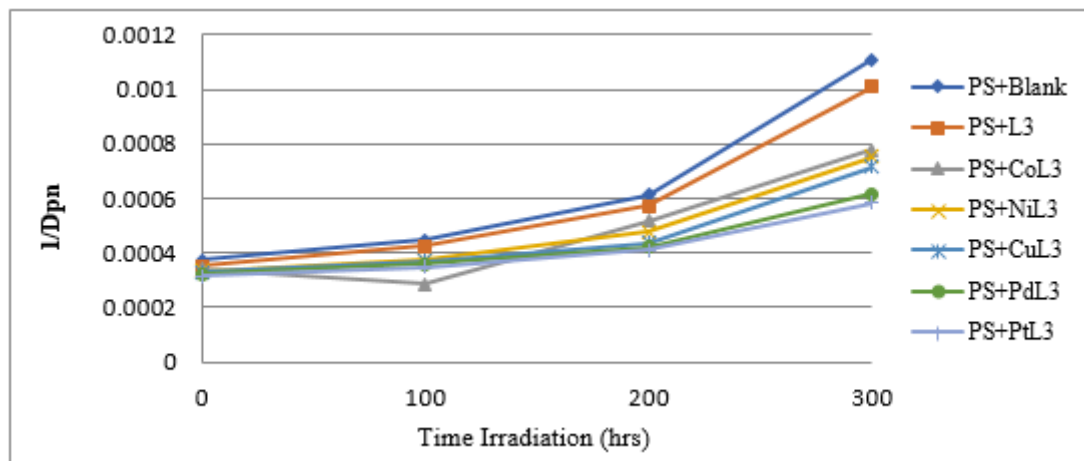


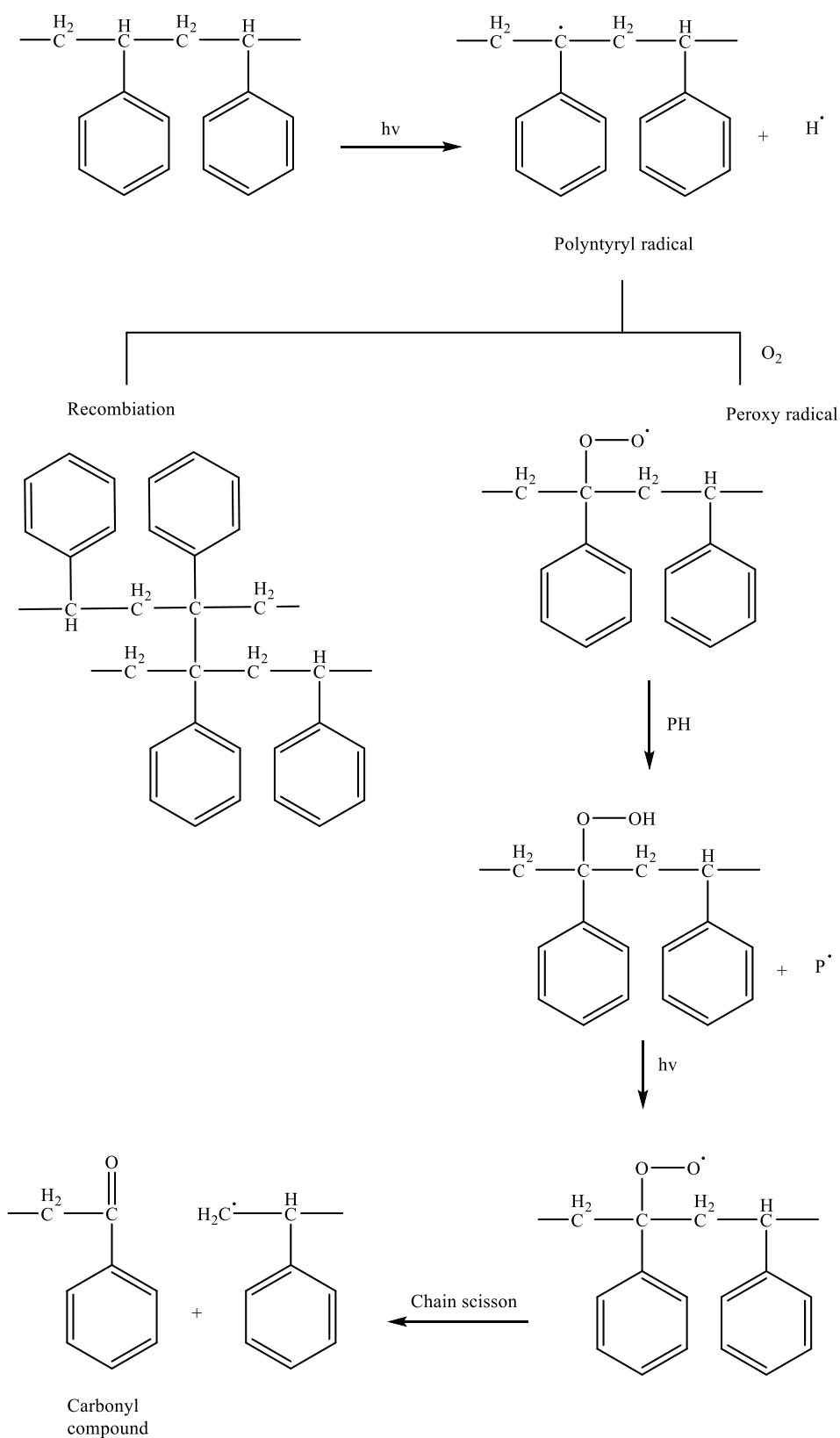
Figure 25: Distinction of  $1 / DP_n$  to the additional PS film irradiance thickness ( $40\mu\text{m}$ ) ( $0.5\text{w} / \text{v}$ )

Reverse polymerizing ( $1 / DP_n$ ) compared with a reversed sample in front of a blank shows an increase in radiation time ( $1 / DP_n$ ) [31].

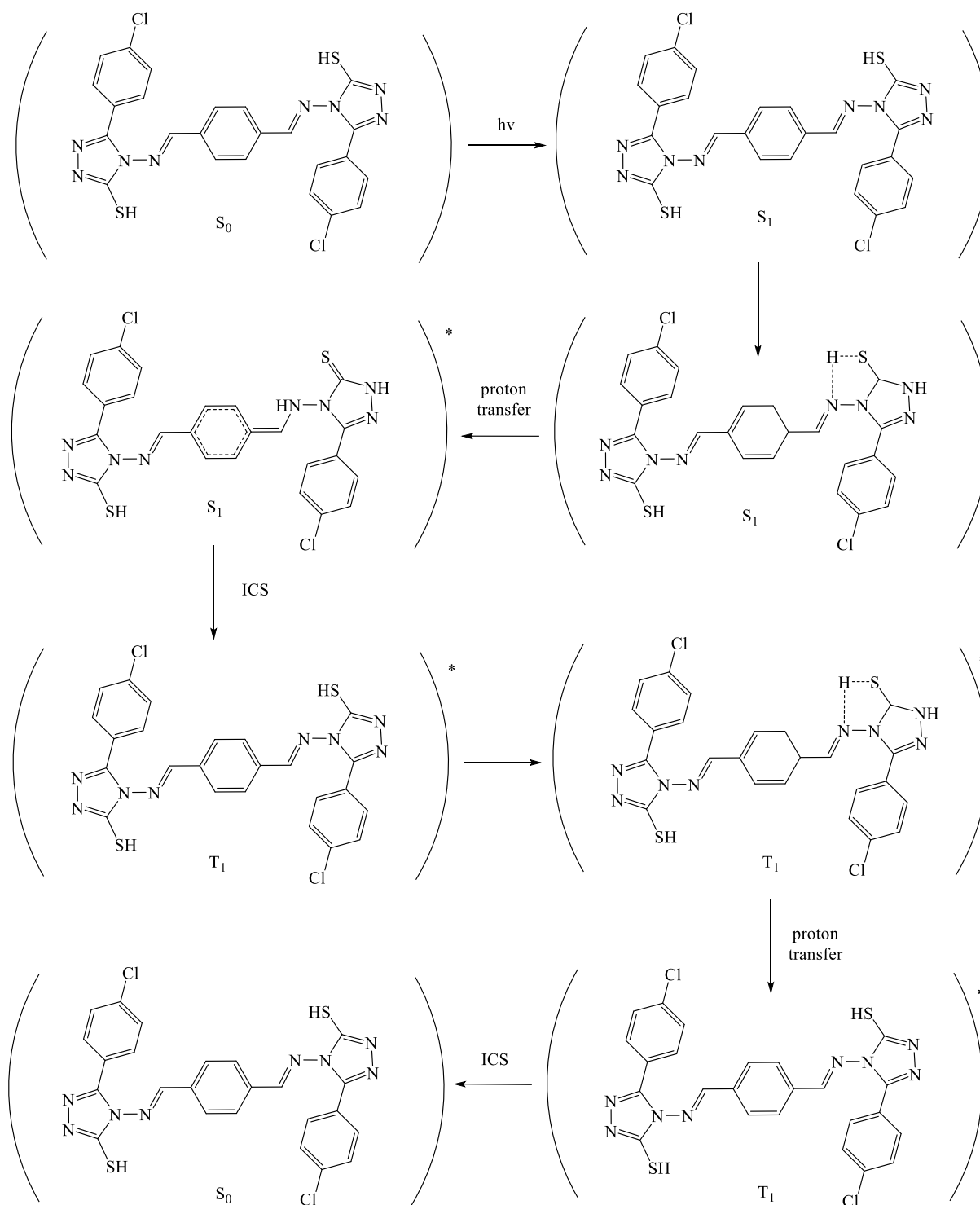
Mechanisms suggested by which the Polystyrene PS additives are stabilized

The ultra-violet-light derivative complexes in 1,2,4-triazole-3-thion induce radical scavenging and peroxide degeneration in polystyrene photography stability, and the 1,2,4-triazole-3-thion ring is critical in photo-stabilization if ultraviolet light absorption exposures lead to an ultraviolet energy decrease in the aromatic ring. The conservation of transmission energy between chelates and chromophore excitations ( $POO\bullet$ ) (Scheme 2, 3), may result in radical

cavities in the complex of microphones. All this movement towards film stabilization by resonance. All commercial polymers are necessary to break down the polymer (C-C) bond result from degradation, when exposed to ultraviolet light permanently. Energy transfer highly impotent in polymers is directly linked to effects of stabilization of the photograph and photodegradation which can occur through the following process (i) inter-molecular transfer energy among photo stabilizer (acceptor) molecules and an exciting polymer (donor) molecule. (ii) Intramolecular energy transfer this process occurs between the molecules of polymer (acceptor) and another thrilling chain (dono) chromophore [32-35].

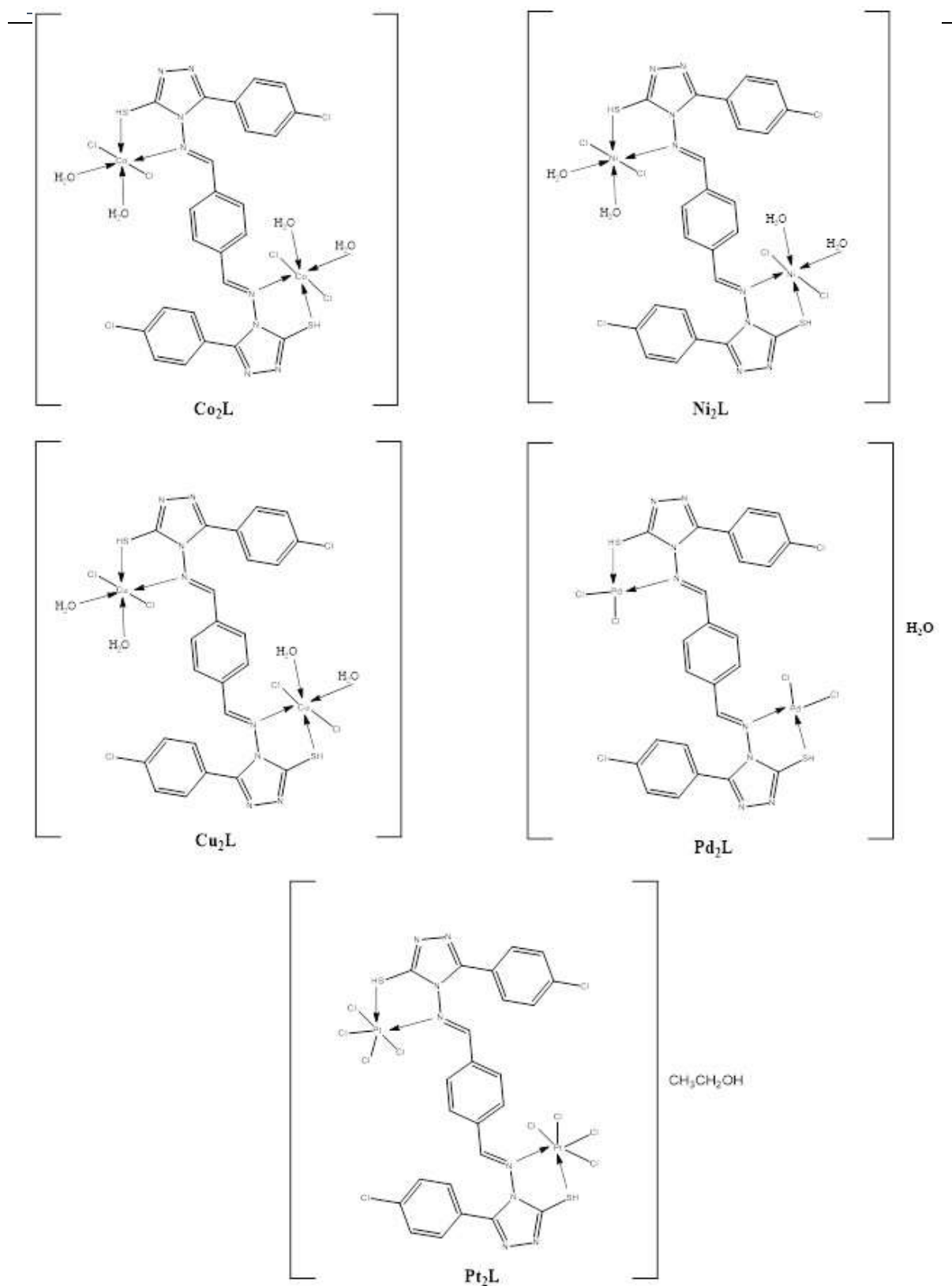


Scheme 2: Polystyrene photooxidation scheme.



Scheme 3: the UV absorption mechanism and energy dissipation as thermal in the Polystyrene Photo Station.





Scheme 4: Suggested structures for all complexes

## CONCLUSION

In the present research work, we synthesized new Schiff base Ligand by condensation substituted [benzene-1,4-dicarboxaldehyde] with compound (5) whose name is [4-amino-5-(4-chlorophenyl)-4H-1,2,4-triazole-3-thione].

This new Schiff base ligand was used to synthesized five metal complexes. The ratio (2:1) between metal to ligand is prevalent in preparing our complexes; The compound of ligand ( $\text{L}_3$ ) Schiff-base (S.B) and complexes have been examined and confirmed by Fourier transform infrared

(FT-IR), *Ultraviolet-visible* (UV-visible), Proton nuclear magnetic resonance (<sup>1</sup>HNMR), carbon<sup>13</sup> nuclear magnetic resonance (<sup>13</sup>CNMR), Magnetic susceptibility, carbon-hydrogen nitrogen sulfur (C–H–N–S), atomic-absorption-flame (AAF), conductivity and thermal-analysis (TG). Coordinates between azomethane group ligand and metal ions and (C = S) groups of sulfurs. Photo-stability and stability for polymer polystyrene were then studied, given the stability of the ligand and complexes by order:

Pt<sub>2</sub>L<sub>3</sub> > Pd<sub>2</sub>L<sub>3</sub> > Cu<sub>2</sub>L<sub>3</sub> > Ni<sub>2</sub>L<sub>3</sub> > Co<sub>2</sub>L<sub>3</sub> > L<sub>3</sub> > PS

The results of weight loss percentage data, mean molecular weight, show improved stability for polystyrene PS.

## REFERENCES

1. Mathur P, Misra S. Metal-carbonyl promoted multicomponent coupling of alkynes for the synthesis of heterocyclic compounds. *advances in Organometallic Chemistry* 2020 Jan 1 (Vol. 73, pp. 253-304). Academic Press
2. Wirtanen T, Rodrigo E, Waldvogel S. Recent Advances in the Electrochemical Reduction of Substrates Involving N-O bonds. *Advanced Synthesis & Catalysis*. 2020 Apr 30
3. Zhang J, Buell J, Chan K, Ibrahim PN, Lin J, Pham P, Shi S, Spevak W, Wu G, Wu J, inventors; Plexikon Inc, assignee. Heterocyclic compounds and uses thereof. United States patent US 10,519,177. 2019 Dec 31
4. Tripathi A, Prabhakar C. Impact of heteroatom (S and N) position and change in central ring of anthracene with heterocyclic ring on charge transport and optical properties in anthratetra-thiazole (ATTz). *Journal of Sulfur Chemistry*. 2019 Jul 4;40(4):361-76.
5. Brinkmann M, Schneider AL, Bluhm K, Schiwiy S, Lehmann G, Deutschmann B, Müller A, Tiehm A, Hollert H. Ecotoxicity of Nitrogen, Sulfur, or Oxygen Heterocycles and Short-Chained Alkyl Phenols Commonly Detected in Contaminated Groundwater. *Environmental toxicology and chemistry*. 2019 Jun;38(6):1343-55.
6. Dwivedi A, Singh S, Kumar S, Mittal PC. Organosulfur phytochemicals against metabolic and neurodegenerative diseases: benefits and risks. *In Phytochemicals as Lead Compounds for New Drug Discovery* 2020 Jan 1 (pp. 179-194). Elsevier
7. Pathan SI, Chundawat NS, Chauhan NP, Singh GP. A review on synthetic approaches of heterocycles via insertion-cyclization reaction. *Synthetic Communications*. 2020 Jan 16:1-35
8. Nahi RJ, Imran NH. Synthesis, Characterization and Thermal Stability Study of New Heterocyclic Compounds Containing 1, 2, 3-Triazole and 1, 3, 4-Thiadiazole Rings. *Oriental Journal of Chemistry*. 2019;35(1):234
9. Sangwan J. Synthesis and Antibacterial Activity of Substituted 1, 2, 3 Triazoles Having Furyl Moiety. Available at SSRN 3534134. 2020 Feb 7
10. Milyushkin AL, Birin KP, Matyushin DD, Semeikin AV, Iartsev SD, Karnaeva AE, Uleanov AV, Buryak AK. Isomeric derivatives of triazoles as new toxic decomposition products of 1, 1-dimethylhydrazine. *Chemosphere*. 2019 Feb 1;217:95-9.
11. Othman AA, Kihel M, Amara S. 1, 3, 4-Oxadiazole, 1, 3, 4-thiadiazole and 1, 2, 4-triazole derivatives as potential antibacterial agents. *Arabian Journal of Chemistry*. 2019 Nov 1;12(7):1660-75
12. Pervaiz M, Ahmad I, Yousaf M, Kirn S, Munawar A, Saeed Z, Adnan A, Gulzar T, Kamal T, Ahmad A, Rashid A. Synthesis, spectral and antimicrobial studies of amino acid derivative Schiff base metal (Co, Mn, Cu, and Cd) complexes. *Spectrochimica Acta Part A: Molecular and Biomolecular Spectroscopy*. 2019 Jan 5;206:642-9.
13. Abdel-Fatah SM, Díaz-Sánchez M, Díaz-García D, Prashar S, Abdel-Rahman LH, Gómez-Ruiz S. Nanostructured Metal Oxides Prepared from Schiff Base Metal Complexes: Study of the Catalytic Activity in Selective Oxidation and C–C Coupling Reactions. *Journal of Inorganic and Organometallic Polymers and Materials*. 2019 Jul 30:1-3
14. Ali AA, Al-Hassani RM, Hussain DH, Rheima AM, Meteab HS. Synthesis, spectroscopic, characterization, pharmacological evaluation, and cytotoxicity assays of novel nano and micro scale of copper (II) complexes against human breast cancer cells. *Drug Invention Today*. 2020 Jan 15;14(1)
15. Ali AA, Al-Hassani RM, Hussain DH, Rheima AM, Abd AN, Meteab HS. Fabrication of Solar Cells Using Novel Micro-and Nano-Complexes of Triazole Schiff Base Derivatives. *Journal of Southwest Jiaotong University*. 2019;54(6)
16. Aswathanarayanappa, C., Bheemappa, E., Bodke, Y. D., Krishnegowda, P. S., Venkata, S. P. & Ningegowda, R. Synthesis and Evaluation of Antioxidant Properties of Novel 1, 2, 4-Triazole-Based Schiff Base Heterocycles. *Archiv der Pharmazie*, 2013; 346, 922-930.
17. Yousif, E., Majeed, A., Al-Sammarae, K., Salih, N., Salimon, J. & Abdullah, B. Metal complexes of Schiff base: preparation, characterization and antibacterial activity. *Arabian Journal of Chemistry*, 2017.10, S1639-S1644.
18. Waaleed, A., Jabbar, S. A. & Jassim, I. K. 2015. Synthesis and study the biological activity of some new heterocyclic compounds. *karbala journal of pharmaceutical sciences*.
19. Al-Shemary, R., Al-Khazraji, A. & Lateef, A. Synthesis, characterization and antimicrobial activity studies of mixed-1, 10-phenanthroline-Mn (II), Co (II), Cu (II), Ni (II) and Hg (II) complexes with schiff base [2, 2'-(1Z, 1'Z)-(biphenyl-4, 4'-diylbis (azan-1-yl-1-ylidene)) bis (methan-1-yl-1-ylidene) diphenol]. *International Journal of Science and Research (IJSR)*, 2016. 5, 1787-1793.
20. Sun, W., Gao, X. & Lu, F. Synthesis and properties of poly-Schiff base containing bisthiazole rings. *Journal of applied polymer science*, 1997.64, 2309-2315.
21. Shaygan, S., Pasdar, H., Foroughifar, N., Davallo, M. & Motiee, F. Cobalt (II) complexes with Schiff base ligands derived from terephthalaldehyde and ortho-

- substituted anilines: synthesis, characterization and antibacterial activity. *Applied Sciences*, 2018. 8, 385.
22. ATB Basim I. Al-Abdali, I. K. J. Synthesis and Characterization of New (2-(((5-(3, 5-Dinitrophenyl)-1, 3, 4-Thiadiazol-2-yl)-2,5 Dihydroxy Benzalidine))) Metal Complexes. *Journal of Global Pharma Techn*, 2019. 11, 39-55.
  23. Nakamoto, K. *Infrared and Raman Spectra of Inorganic and Coordination Compounds*, 19972 Volume Set, Wiley.
  24. Al-Shemary, R. K., Al-khazraji, A. M. & Niseaf, A. N. Preparation, spectroscopic study of Schiff base ligand complexes with some metal ions and evaluation of antibacterial activity. *The Pharma Innovation*, 2016. 5, 81.
  25. Re.DENNEY, G. H. J. B. J. M. *Vogel's Quantitative Chemical Analysis*, Pearson Education India, 2009.
  26. AWAD, A. A., AL-HASANI, R. A., YOUSIF, E. A. & IBRAHIM, S. K. SYNTHESIS, CHARACTERIZATION AND THEORETICAL STUDIES OF [(4-AMINO-5-(2-(6-METHOXYNAPHTHALEN-2-YL) PIPERIDINO)-1, 2, 4-TRIAZOLE-3-THION] WITH Co (II), Ni (II), Cu (II), Zn (II) and Cd (II) METAL IONS. *Acta Chim. Pharm. Indica*, 2015.5, 107-120.
  27. Zan, L., Wang, S., Fa, W., Hu, Y., Tian, L. & Deng, K. Solid-phase photocatalytic degradation of polystyrene with modified nano-TiO<sub>2</sub> catalyst. *Polymer*, 2006.47, 8155-8162.
  28. Rabie, S. T., Ahmed, A. E., Sabaa, M. W. & El-Ghaffar, M. A. Maleic diamides as photostabilizers for polystyrene. *Journal of Industrial and Engineering Chemistry*, 2013.19, 1869-1878.
  29. Potts, J., Clendinning, R., Ackart, W. & Niegisch, W. *Polymers and Ecological Problems*. ed. Guillet JE, Plenum Press, New York, 1973.61-79.
  30. Shyichuk, A. & White, J. 2000. Analysis of chain-scission and crosslinking rates in the photo-oxidation of polystyrene. *Journal of Applied Polymer Science*, 77, 3015-3023.
  31. Allen, N. S., Luc-Gardette, J. & Lemaire, J. Photostabilising action of ortho-hydroxy benzophenones in polypropylene film: influence of processing and wavelength of irradiation. *Polymer Photochemistry*, 1983. 3, 251-265.
  32. Ali, G. Q., El-Hiti, G. A., Tomi, I. H. R., Haddad, R., Al-Qaisi, A. J. & Yousif, E. Photostability and performance of polystyrene films containing 1, 2, 4-triazole-3-thiol ring system Schiff bases. *Molecules*, 2016. 21, 1699.
  33. Bakir, E. T., Hameed, A. S. & Yousif, E. A. Synthesis and photochemical study of poly (vinyl chloride)-1, 3, 4-oxadiazole and 1, 3, 4-thiadiazole. *Al-Nahrain Journal of Science*, 2007.10, 7-12.
  34. El-Hiti, G. A., Alotaibi, M. H., Ahmed, A. A., Hamad, B. A., Ahmed, D. S., Ahmed, A., Hashim, H. & Yousif, E. The morphology and performance of poly (vinyl chloride) containing melamine Schiff bases against ultraviolet light. *Molecules*, 2019. 24, 803.
  35. Yousif, E. A., ALIWI, S. A., Ameer, A. A. & Ukal, J. R. Improved photostability of PVC films in the presence of 2-thioacetic acid-5-phenyl-1, 3, 4-oxadiazole complexes. *Turkish Journal of Chemistry*, 2009.33, 399-410.